ORIGINAL ARTICLE

Journal of Cachexia, Sarcopenia and Muscle 2021; **12**: 1704–1723
Published online 23 August 2021 in Wiley Online Library (wileyonlinelibrary.com) **DOI:** 10.1002/jcsm.12767

TMEM182 interacts with integrin beta 1 and regulates myoblast differentiation and muscle regeneration

Wen Luo[1,2,3,5], Zetong Lin[2,3], Jiahui Chen[2,3], Genghua Chen[2,3], Siyu Zhang[2,3], Manqing Liu[1,2,3], Hongmei Li[1,2,3], Danlin He[1,2,3], Shaodong Liang[1,2,3], Qingbin Luo[1,2,3], Dexiang Zhang[1,2,3], Qinghua Nie[1,2,3,4]* & Xiquan Zhang[1,2,3,4]*

[1]*Lingnan Guangdong Laboratory of Agriculture, South China Agricultural University, Guangzhou, China;* [2]*Department of Animal Genetics, Breeding and Reproduction, College of Animal Science, South China Agricultural University, Guangzhou, China;* [3]*Guangdong Provincial Key Lab of Agro-Animal Genomics and Molecular Breeding, and Key Lab of Chicken Genetics, Breeding and Reproduction, Ministry of Agriculture and Rural Affair, South China Agricultural University, Guangzhou, China;* [4]*State Key Laboratory for Conservation and Utilization of Subtropical Agro-Bioresources, South China Agricultural University, Guangzhou, China;* [5]*Department of Orthaepedics and Traumatology, The Chinese University of Hong Kong, Hongkong*

Abstract

Background Transmembrane proteins are vital for intercellular signalling and play important roles in the control of cell fate. However, their physiological functions and mechanisms of action in myogenesis and muscle disorders remain largely unexplored. It has been found that *transmembrane protein 182* (*TMEM182*) is dramatically up-regulated during myogenesis, but its detailed functions remain unclear. This study aimed to analyse the function of *TMEM182* during myogenesis and muscle regeneration.

Methods RNA sequencing, quantitative real-time polymerase chain reaction, and immunofluorescence approaches were used to analyse *TMEM182* expression during myoblast differentiation. A dual-luciferase reporter assay was used to identify the promoter region of the *TMEM182* gene, and a chromatin immunoprecipitation assay was used to investigate the regulation *TMEM182* transcription by MyoD. We used chickens and *TMEM182*-knockout mice as *in vivo* models to examine the function of *TMEM182* in muscle growth and muscle regeneration. Chickens and mouse primary myoblasts were used to extend the findings to *in vitro* effects on myoblast differentiation and fusion. Co-immunoprecipitation and mass spectrometry were used to identify the interaction between *TMEM182* and integrin beta 1 (ITGB1). The molecular mechanism by which *TMEM182* regulates myogenesis and muscle regeneration was examined by Transwell migration, cell wound healing, adhesion, glutathione-S-transferse pull down, protein purification, and RNA immunoprecipitation assays.

Results *TMEM182* was specifically expressed in skeletal muscle and adipose tissue and was regulated at the transcriptional level by the myogenic regulatory factor MyoD1. Functionally, *TMEM182* inhibited myoblast differentiation and fusion. The *in vivo* studies indicated that *TMEM182* induced muscle fibre atrophy and delayed muscle regeneration. *TMEM182* knockout in mice led to significant increases in body weight, muscle mass, muscle fibre number, and muscle fibre diameter. Skeletal muscle regeneration was accelerated in *TMEM182*-knockout mice. Furthermore, we revealed that the inhibitory roles of *TMEM182* in skeletal muscle depend on ITGB1, an essential membrane receptor involved in cell adhesion and muscle formation. *TMEM182* directly interacted with ITGB1, and this interaction required an extracellular hybrid domain of ITGB1 (aa 387–470) and a conserved region (aa 52–62) within the large extracellular loop of *TMEM182*. Mechanistically, *TMEM182* modulated ITGB1 activation by coordinating the association between ITGB1 and laminin and regulating the intracellular signalling of ITGB1. Myogenic deletion of *TMEM182* increased the binding activity of ITGB1 to laminin and induced the activation of the FAK-ERK and FAK-Akt signalling axes during myogenesis.

Conclusions Our data reveal that *TMEM182* is a novel negative regulator of myogenic differentiation and muscle regeneration.

Keywords *TMEM182*; Myogenesis; Muscle regeneration; Integrin beta 1; FAK signalling

Received: 1 March 2021; Revised: 28 May 2021; Accepted: 10 July 2021
**Correspondence to: Qinghua Nie and Xiquan Zhang, Department of Animal Genetics, Breeding and Reproduction, College of Animal Science, South China Agricultural University, Guangzhou 510642, China. Email: nqinghua@scau.edu.cn; xqzhang@scau.edu.cn*

Introduction

Skeletal muscle constitutes approximately 35% of the body weight and plays important roles in the support, movement, and homeostasis of organisms.[1] Skeletal muscle is composed of a series of muscle fibres made of muscle cells. These muscle cells are multinucleated and form during development through the fusion of several undifferentiated cells called myoblasts into long and multinucleated myotubes.[2] The number of muscle fibres remains constant after birth, but each muscle fibre fuses with satellite cells, a population of adult stem cells responsible for skeletal muscle regeneration and growth. After an injury, the population of satellite cells can be activated to generate myoblasts that proliferate and differentiate into multinucleated myotubes. The process of myoblast proliferation and the differentiation is called myogenesis and is not only important for muscle development and growth but also necessary for muscle regeneration.

It is well known that membrane proteins, which constitute approximately 30% of the proteome, play critical roles in many biological processes, such as transport, signalling, and intercellular communication.[3,4] Notably, many of these processes are involved in myogenesis, indicating that membrane proteins play critical roles in muscle.[5] Transmembrane proteins span the entirety of the cell membrane. The transmembrane (TMEM) protein family includes proteins with mostly unknown functions. As research on TMEM family members has continued, many functions and mechanisms of TMEM proteins have been revealed. However, only a few TMEM proteins have been reported to play a role during skeletal muscle development. To date, only four TMEM proteins have been reported to be involved in the regulation of muscle physiology. The calcium-activated chloride channel *TMEM16A* plays crucial roles in numerous physiological processes, including neuronal excitability, smooth muscle contraction, transepithelial secretion, and intestinal motility.[6] In skeletal muscle, *TMEM16A* is robustly expressed and is critical for action potential acceleration.[5] However, its roles in myogenesis and muscle disorder have never been reported. *TMEM2* is essential for the regulation of skeletal muscle morphogenesis. Loss of *TMEM2* in muscle tissue results in destabilization of muscle fibres.[7] *TMEM8C*, also called Myomaker or Mymk, is a membrane activator of myoblast fusion and plays crucial roles in muscle formation and regeneration.[8–10] By using RNA sequencing (RNA-seq) analysis, we found that the expression of *TMEM182* was up-regulated during myogenesis; a previous study also showed that this gene may be involved in muscle development,[11] but its specific roles in muscle remain unknown.

In the present study, we identified and characterized *TMEM182* in skeletal muscle using chickens and mice as animal model. *TMEM182*, which can be directly regulated by MyoD1, was found to be specifically expressed in muscle and adipose tissue. The *in vitro* and *in vivo* experimental results demonstrated the inhibitory roles of *TMEM182* in skeletal muscle development, growth, and regeneration. Additionally, we found that the inhibitory roles of *TMEM182* in skeletal muscle were dependent on its direct interaction with integrin beta 1 (ITGB1). Taken together, our results provide a structural framework for understanding the expression, regulation, and function of *TMEM182* in skeletal muscle and suggest a critical candidate gene for elucidating the mechanisms underlying muscle development, growth, and regeneration.

Methods

Ethics standards

All experimental protocols were approved by the South China Agricultural University Institutional Animal Care and Use Committee (approval number: SCAU-2018f052). And the methods were carried out in accordance with the regulations and guidelines established by this committee.

Cell culture

Chicken primary myoblasts were isolated from the chicken leg and breast muscle of day 10 embryo as previous described.[12] Primary myoblast represented the chicken primary myoblasts that have just completed serial plating. Growing myoblast represented myoblasts that were cultured in growth medium with RPMI-1640 (Gibco, Grand Island, NY, USA), 15% foetal bovine serum (FBS) (ExCell, Shanghai, China), 10% chicken embryo extract, and 0.2% penicillin/streptomycin (Gibco) at 37°C in 5% CO_2. Differentiated myotube (DM) represented myoblasts induced to differentiation for 4 days by culturing the cells in differentiation medium (RPMI-1640 without FBS containing 2% horse serum) when 90% confluent.

Mouse primary myoblasts were isolated and cultured as previously described.[13] Cells were isolated from the forelimbs and hindlimbs of 3-week-old mice, minced and digested in a solution of dispase B and type I collagenase. Growth medium consisted of Ham's F-10 nutrient mixture (Gibco) supplemented with 20% FBS (ExCell) and 2.5 ng/mL bFGF (Promega, Madison, WI, USA). Differentiation medium consisted of DMEM (Gibco) supplemented with 2% horse serum (Gibco). All medium contained 0.2% penicillin/streptomycin (Gibco).

RNA extraction, cDNA synthesis, and quantitative real-time PCR

Total RNA was extracted from tissues or cells using RNAiso reagent (Takara, Otsu, Japan). Reverse transcription reaction

DOI: 10.1002/jcsm.12767

for mRNA was performed with PrimeScript™ RT reagent Kit (Perfect Real Time) (Takara) according to the manufacturer's manual. The specific mRNA PCR Primers were designed and provided in Supporting Information, *Table* S3. Quantitative real-time polymerase chain reaction (qPCR) programme was carried out in ABI QuantStudio 5 qPCR System (Applied Biosystem Inc., Foster City, CA, USA), following the method as described.[14] All reactions were run in triplicate.

RNA sequencing

For chicken myoblast RNA-seq, the chicken primary myoblast (cultured in growth medium for 1 h), growing myoblast (50% confluence, cultured in growth medium), and DM (100% confluence, cultured in differentiation medium for 4 days) were harvested and total RNA was extracted using RNAiso reagent (Takara). Then, the RNA samples were sent to Beijing Novogene Bioinformation Technology Co., Ltd. (China) for RNA-seq. Paired-end RNA-seq was performed using the Illumina HiSeq 2000 platform (Illumina, San Diego, CA, USA) to obtain 101 bp reads. Raw read quality was assessed using the FastQC suite version 0.10.1. Raw reads were processed with custom perl scripts to remove reads containing adapter, reads containing poly-N and low-quality reads. All the downstream analyses were based on the clean data with high quality based on a rerun of FastQC. The RNA-seq reads were aligned using HISAT, mapped to the reference genome based on the NCBI *Gallus gallus* Build 6.0 (Ensemble V96). HTSeq was used to count the read numbers mapped to each gene. The FPKM (fragments per kilobase of exon per million mapped fragments) values were used to estimate the gene expression levels, and differentially expressed genes (DEGs) between two samples were identified with DESeq using the criteria false-discovery rate (FDR) < 0.01, $|\log2FC| \geq 0.5$, and padj ≤ 0.05. All the sequence data have been deposited in NCBI's Gene Expression Omnibus (GEO, http://www.ncbi.nlm.nih.gov/geo) and are accessible through GEO series accession number GSE148017.

For mice RNA-seq, gastrocnemius muscle from the *TMEM182*-knockout (KO) and wild-type (WT) mice were harvested and total RNA were extracted using RNAiso reagent (Takara). High-throughput RNA-seq was performed on the BGISEQ-500 platform (BGI, Wuhan, China) with 100 bp paired-end sequencing length. The high-quality clean reads generated by BGISEQ-500 platform were mapped to the PacBio reference transcriptome by Bowtie2 (v2.2.5), then the transcript expression level was calculated and normalized to FPKM using RSEM software (v1.2.8). The significance of the DEGs was defined by the bioinformatics service of BGI according to the DEGseq. FDR < 0.01, $|\log2FC| \geq 0.5$, padj ≤ 0.05 was set as the threshold for selection of differentially expressed gene. All the sequence data have been deposited in GEO and are accessible through GEO series accession number GSE148019. Kyoto Encyclopedia of Genes and Genomes pathway enrichment analysis of DEGs was evaluated using the database for annotation, visualization, and integrated discovery (https://david.ncifcrf.gov). Enriched pathways were identified according to the default settings of database for annotation, visualization, and integrated discovery. Pathways associated with human diseases or cancers were not included. Gene expression data of RNA-seq were analysed using gene-set enrichment analysis (GSEA) (http://www.broadinstitute.org/gsea/index.jsp). By default, the FDR < 0.25 is significant in GSEA.

Immunoblotting

Western blot was performed as previously described.[15] The following antibodies were used: anti-TMEM182 (1:500, chicken and mice anti-TMEM182 monoclonal antibody was customized by Abmart (Shanghai, China), this antibody was synthesized in response to the injection of recombinant chicken or mice TMEM182 protein into mouse), anti-p38α (1:300, sc-271120, Santa Cruz Biotechnology, CA, USA), anti-p-p38 (detection of Tyr 182 phosphorylated p38. 1:300, sc-166182, Santa Cruz Biotechnology), anti-ERK1 (1:300, sc-376852, Santa Cruz Biotechnology), anti-p-ERK (detection of ERK phosphorylated at Tyr 204. 1:300, sc-7383, Santa Cruz Biotechnology), anti-p-JNK (detection of Thr 183 and Tyr 185 phosphorylated JNK. 1:300, sc-6254, Santa Cruz Biotechnology), anti-ITGB1 (1:400, sc-53711, Santa Cruz Biotechnology), anti-ITGA7 (1:400, sc-515716, Santa Cruz Biotechnology), anti-FLAG (1:5000, A02010, Abbkine, Guangzhou, China), anti-Laminin β1 (1:400, sc-17810, Santa Cruz Biotechnology), anti-focal adhesion kinase (FAK) (1:1000, 610087, BD Biosciences, San Jose, USA), anti-p-FAK (detection of Y861 phosphorylated FAK. 1:1000, ab200811, Abcam, Cambridge, USA), anti-AKT1 (1:1000, ab227385, Abcam), anti-p-AKT1 (detection of Ser 473 phosphorylated Akt1. 1:400, sc-52940, Santa Cruz Biotechnology), anti-glutathione-S-transferse (GST) (1:5000, sc-138, Santa Cruz Biotechnology), and anti-Tubulin (1:10000, BS1482M, Bioworld, Beijing, China).

Immunofluorescence

The immunofluorescence was performed using anti-MyHC (1:50, B103, DSHB, Iowa City, USA) and anti-TMEM182 (1:200, Abmart). The cell nuclei were stained for DAPI (Beyotime, Jiangsu, China) or Hoechst (Beyotime). Total myotube area was calculated as the percentage of the total image area covered by myotubes, and the measurement was performed using ImageJ software (National Institutes of Health, Bethesda, MD) on cells labelled with anti-MyHC. To stain live cells, we washed the cells with phosphate-buffered

saline (PBS) and incubated them in blocking buffer (3% bovine serum albumin/PBS) for 15 min. Incubation of anti-TMEM182 was then performed on ice, followed by fixation with 4% PFA/PBS and incubation with secondary antibody. These cultures were visualized on a Leica TCS SP8 confocal microscope.

Generation of TMEM182-knockout mice and phenotype measurements

TMEM182-KO mice were generated using the clustered regularly interspaced short palindromic repeats (CRISPR) genome-editing system in the C57BL/6 background by Cyagen Biosciences. Briefly, a pair of single-guide RNAs (sgRNAs) (sgRNA1: CGATGTTCTTAGTCTCAACGAGG and sgRNA2: ACTAGATGAAACCGTAGGTGTGG) were designed using an online CRISPR design tool (http://tools.geneome-engineering.org) to delete a 2517 bp genomic region containing exon 2, intron 2, and exon3 of mice *TMEM182* gene, and the sgRNAs were inserted into the px459 vector (Addgene, Cambridge, MA, USA). The purified sgRNA-Cas9-px459 vector was injected into fertilized eggs, and successful KO was validated by PCR amplification with *TMEM182* specific primers: forward primer, 5′-TCATTTGGAAGGCAACCAGTCG-3′; reverse primer, 5′-GTCACATGGAGGTTGGAGGTTC-3′. WT mice had an amplicon of 3096 bp, while KO mice possessed an amplicon of 579 bp. The founder mice were randomly mated to produce offspring for additional studies. Male and female KO and WT offspring mice were randomly selected, and their body weights were measured weekly. The gastrocnemius, tibialis anterior, and quadriceps muscles of KO and WT mice were collected and weighed at 9 weeks of age. Mice were euthanized by cervical dislocation. Before euthanized, pentobarbital sodium (Guoyao, Beijing, China) was injected intraperitoneally at a dose of 50 mg/kg to anesthetize the mice.

Muscle injury and regeneration

For chicken muscle injury and regeneration, muscle injury was induced in 3-week-old chick by injecting 50 μL of 50 mM $BaCl_2$ in PBS into the gastrocnemius muscle. Muscles were then harvested at the indicated days after injection to assess the regeneration and repair. Chickens were euthanized by cervical dislocation. Before euthanized, pentobarbital sodium was injected intravenously at a dose of 30 mg/kg to anesthetize the chickens.

For mice muscle injury and regeneration, mice were anesthetized by intraperitoneal injection of pentobarbital sodium at 50 mg/kg prior to muscular injection. Muscle injury was induced in 9-week-old male and female mice by injecting 50 μL of 10 mM cardiotoxin (CTX) (Sigma, St. Louis, MO, USA) in PBS into the gastrocnemius muscle. Muscles were then harvested at the indicated days after injection to assess the regeneration and repair. Mice were euthanized by cervical dislocation. Before euthanized, pentobarbital sodium was injected intraperitoneally at a dose of 50 mg/kg to anesthetize the mice.

Muscle atrophy

Chicken muscle atrophy was induced in 3-week-old chick by injecting dexamethasone (750 μg/kg body weight) into the gastrocnemius muscle once a day for 3 days. Muscles were then harvested at the indicated days after injection to assess the atrophy. Chickens were euthanized by cervical dislocation. Before euthanized, pentobarbital sodium was injected intravenously at a dose of 30 mg/kg to anesthetize the chickens.

Histology

Skeletal muscle samples were harvested and fixed with 10% formalin in PBS. Fixed tissues were paraffin-embedded, sectioned, and stained with haematoxylin and eosin (H&E). Images were acquired using an optical microscope (Leica, Wetzlar, Germany). For lentivirus mediated *TMEM182* overexpression *in vivo* assay, we harvested the gastrocnemius muscle around the lentivirus injection site to analyse the cross-sectional area (CSA) of each muscle fibre. The collected muscle samples were transected to obtain cross-sections. At least five randomly selected non-overlapping images were acquired for each cross-section, and the CSA of almost all muscle fibres (except for the fibres with blurred outlines that could not be recognized by the software) in each image was measured. We used the mean value of all muscle fibre CSAs obtained in the five images as the 'average CSA' of the muscle in this sample. The CSAs and diameters of individual myofibres were quantified using NIS-Elements BR software (Nikon, Tokyo, Japan). For studies in WT and *TMEM182*-KO mice, cross-sections of gastrocnemius muscle were imaged with a living cell workstation (Leica), and the total muscle fibre number was quantified using ImageJ.

Plasmid construction

Gene overexpression vector: *TMEM182* coding sequence (NCBI Reference Sequence: XM_416920.6), *MyoD1* coding sequence (NCBI Reference Sequence: NM_204214.2), and *ITGB1* coding sequence (NCBI Reference Sequence: NM_001039254.2) were amplified from chicken embryonic leg muscle cDNA by PCR. PCR product was cloned into the pcDNA3.1 vector (Invitrogen). The successful overexpression vector was confirmed by double digesting and DNA sequencing.

DOI: 10.1002/jcsm.12767

TMEM182 overexpression lentivirus vector: *TMEM182* coding sequence was amplified and the PCR product was cloned into the pWPXL vector (Addgene) between *BamH*I and *Eco*RI sites. The successful *TMEM182* overexpression lentivirus vector was confirmed by double digesting and DNA sequencing.

TMEM182 promoter-reporter plasmid: A 2.5 kb fragment of the *TMEM182* promoter was isolated by PCR using the primers listed in *Table* S3. After the PCR product was digested with *Kpn*I and *Xho*I, the insertion was ligated into the pGL3-basic vector (Promega, Madison, WI, USA) to create the expression vector pGL3-R1. After pGL3-R1 was sequenced, this construct was used as a template, and pGL3-R2, pGL3-R3, pGL3-R4, or pGL3-R5 were isolated by PCR. Site-directed mutagenesis of E-box 1 and E-box 2 was carried out by PCR amplification and DpnI digestion to remove the parental DNA.

Dual-luciferase reporter assay

For *TMEM182* promoter assays, chicken primary myoblasts were transfected with reporter plasmid or co-transfected with overexpression vectors for *MyoD1*, and the TK-Renilla reporter (Promega) was co-transfected to each sample as an internal control. After 48 h transfection, cells were washed by PBS twice and the activities of Firefly and Renilla luciferase were measured by Synergy Neo2 HTS Multi-Mode Microplate Reader (Biotek, Winooski, VT, USA) according to the manual of Dual-luciferase reporter assay system (Promega).

Chromatin immunoprecipitation assays

Chromatin immunoprecipitation (ChIP) assays were performed as previously described.[15] Immunoprecipitation was performed with 5 μg of the anti-MyoD1 (554130, BD Biosciences, San Jose, CA, USA) or the chicken anti-IgG (bs-0310P, Bioss) antibody was bound to Protein A/G-Sepharose beads. After extensive washing and reversal of crosslinking, proteinase K and RNase A digestion, chromatin fragments were purified by phenol-chloroform extraction, and ethanol precipitation was performed. The purified DNA was amplified by qPCR. The primer sequences for ChIP-qPCR analysis are shown in *Table* S3.

RNA oligonucleotides and cell transfection

Small interfering RNA (siRNA) against chicken *TMEM182* and *ITGB1* were designed and synthesized by Ribobio (Guangzhou, China), and a nonspecific duplex was used as the control. Transfection was carried out using Lipofectamine 3000 reagent (Invitrogen, Carlsbad, CA, USA). Cells were transfected with 100 nM siRNA (Ribobio, Guangzhou, China). Lipofectamine 3000 and nucleic acids were diluted in OPTI-MEM I Reduced Serum Medium (Gibco). The procedure of transfection was performed according to the manufacturer's direction.

Adhesion assays

Myoblasts (1×10^4) were seeded into the matrigel^{tm} (2 mg/ml, BD Biosciences) pre-coated 96-well plate, and incubated at 37°C for 1 h. After rinsed, attached cells were stained with 0.1% crystal violet and evaluated by measuring the absorbance at 595 nm in a Microplate reader (Bio-rad).

Cell wound healing assay

An approximately 400 μm scratch was made using a sterile pipette tip on a fully confluent cell monolayer 12 h after transfection. Then, the cells were washed and cultured in growth media. Images were taken using a Leica living cell workstation (TCS SP8, Leica). The wound healing effect was calculated as the ratio of the remaining cell-free area to that of the initial wound by using ImageJ.

Transwell migration assay

A total of 5×10^4 cells in 250 μL sera-free media were seeded in an upper chamber of a non-coated Transwell insert (24-well insert; pore size, 8 μm; BD Biosciences). Media supplemented with serum was used as the chemoattractant in the lower chamber. After 24 h incubation, cells in the upper chamber were removed with a cotton swab and cells which migrated through the pores were fixed and stained with DAPI (Beyontime). Images of migrated cells were taken with a fluorescence microscope (Nikon), and the numbers of migrated cells were quantified with ImageJ (National Institutes of Health).

Lentivirus production and transduction

A mixture of pWPXL-*TMEM182* overexpression vector, psPAX2, and pMD2.G were transfected into HEK293T cells using Lipofectamin 3000 reagent to generate lentivirus. The supernatants were collected 72 h later and filtered through 0.45 μm PVDF membranes (Millipore, CA, USA) and cleared by supercentrifugation. The viral titre was evaluated by a gradient dilution. Chicks at the indicated days were infected with lentiviruses (1×10^7 infection unit per chick) by direct injection into the gastrocnemius muscle.

Protein purification and glutathione-S-transferse pulldown

The pGEX-4-T-1-TMEM182, pGEX-4-T-1-ITGB1, or empty pGEX-4-T-1 were transformed into *Escherichia coli* BL21DE3 pLys (Thermo, San Jose, CA, USA). Bacteria were grown to an OD600 of 0.8 and then induced with 0.5 mM of IPTG (Sigma) for 2 h at 37°C in a shaking incubator. TMEM182-GST protein and ITGB1-GST protein were isolated using a GST spin purification kit (Thermo). TMEM182-GST and ITGB1-GST were incubated with total proteins extracted from indicated treated chicken myoblasts or control chicken myoblasts and rotated overnight at 4°C in binding/washing buffer [50 mm Tris (pH 7.5), 0.1 mm Ethylenediaminetetraacetic acid, 1% Triton X-100, 10% glycerol, 1 mm phenylmethylsulfonyl fluoride, and 1 mm DTT]. To pull down GST, Glutathione agarose beads (Thermo) were added the next day and allowed to incubate for 2 h at 4°C and then washed with the washing buffer. Samples were eluted by incubation with Laemmli sample buffer (Bio-rad, CA, USA) and boiling for 5 min. Samples were resolved by sodium dodecyl sulphate polyacrylamide gel electrophoresis. Immunoblotting was performed against FLAG (1:5000, A02010, Abbkine, Guangzhou, China) to detect FLAG-tagged protein and against GST to detect GST protein as a loading control.

Co-immunoprecipitation and mass spectrometry

For immunoprecipitation, lysate containing 1 μg of total protein was precleared using the appropriate isotype IgG antibody, mixed with 2 mg of anti-TMEM182 or anti-ITGB1, then incubated with gentle shaking overnight at 41°C. Protein G agarose (Thermo) was added to each tube and the samples were incubated again with gentle shaking at 41°C. The immunocomplex was washed with cold radioimmunoprecipitation assay buffer and the antibody-selected proteins were eluted from the agarose beads by boiling in SDS-loading buffer (0.1 M Tris–HCl, 10% glycerol, 2% SDS, 0.05% bromophenol blue, and 0.1 M DTT) for 5 min. Each sample was resolved on a 10% SDS–PAGE and visualized with mass spectrometry-compatible silver staining (Invitrogen). Similar conditions with chicken IgG antibody (Bioss) were used for the control lane of each gel. Mass spectrometry analyses were performed in an LC–MS/MS system (Ekspert™ nanoLC, ABSciex Triple TOF™ 5600-plus), and the data analysis was using Proteinpilot software version 4.01 (ABSciex, Massachusetts, USA). We set confidence $\geq$ 95% and Unique peptides $\geq$ 1 as the peptide search condition.

Statistical analysis

Statistical significance was determined by (i) for comparisons among multiple groups, one-way or two-way analysis of variance with Tukey's multiple comparison test was used to compare differences in mean values at the 5% significance level and (ii) for statistical analysis of two contrast, we use two-sided Student's *t*-test. Data were plotted using GraphPad Prism 7 software as mean values, with error bars representing standard error of mean. Representative western blot results were shown from three biologically independent experiments. We considered $P < 0.05$ to be statistically significant. $^{*}P < 0.05$; $^{**}P < 0.01$; $^{***}P < 0.001$.

Results

In vitro *and in vivo characterization of TMEM182 expression in skeletal muscle*

To systematically identify genes involved in myogenesis, we used RNA-seq to identify DEGs during chicken primary myoblast proliferation and differentiation. A total of 6568 genes were significantly differentially expressed among the proliferation and differentiation processes (*Figure* 1A, *Table* S1). Next, we used RNA-seq results from different chicken tissues (data from GSE93855) to identify which of the 6568 DEGs were expressed specifically in skeletal muscle. In total, 189 genes were specifically expressed in skeletal muscle (*Figure* S1), and 57 of these were differentially expressed between the myoblasts at different developmental stages (*Figure* S2). Notably, many well-documented muscle-specific genes with crucial roles in myogenesis, such as *KLHL40*, *MYF5*, *MYF6*, *MYOD1*, and *MYOG*, were included in this set of 57 genes. Expression of the *KLHL40*, *MYF5*, *MYF6*, *MYOD1*, and *MYOG* genes was confirmed by real-time qPCR (*Figure* S3). Interestingly, only one gene encoding a TMEM family protein, *TMEM182*, was among the 57 identified genes. *TMEM182* expression was gradually up-regulated during both chicken myoblast differentiation (*Figure* 1B–1C) and mouse C2C12 myoblast differentiation (*Figure* 1D). Immunocytochemistry of fixed and permeabilized chicken primary myoblasts showed localization of TMEM182 to intracellular vesicle, as expected for a membrane protein (*Figure* 1E). By live cell staining, a common method used to detect plasma membrane proteins, *TMEM182* was detected on the surface of fused myotubes but not in freshly isolated myoblasts (*Figure* 1F). Additionally, *TMEM182* was specifically expressed in muscle and adipose tissues in chickens (*Figure* 1G–1H), and this expression pattern was also found in mammals (*Figure* S4).

Next, we used different muscle samples to study the relevance of *TMEM182* in skeletal muscle development. Our previous RNA-seq results showed that *TMEM182* was more highly expressed in the skeletal muscle of chickens with a lower body weight and slower growth rate

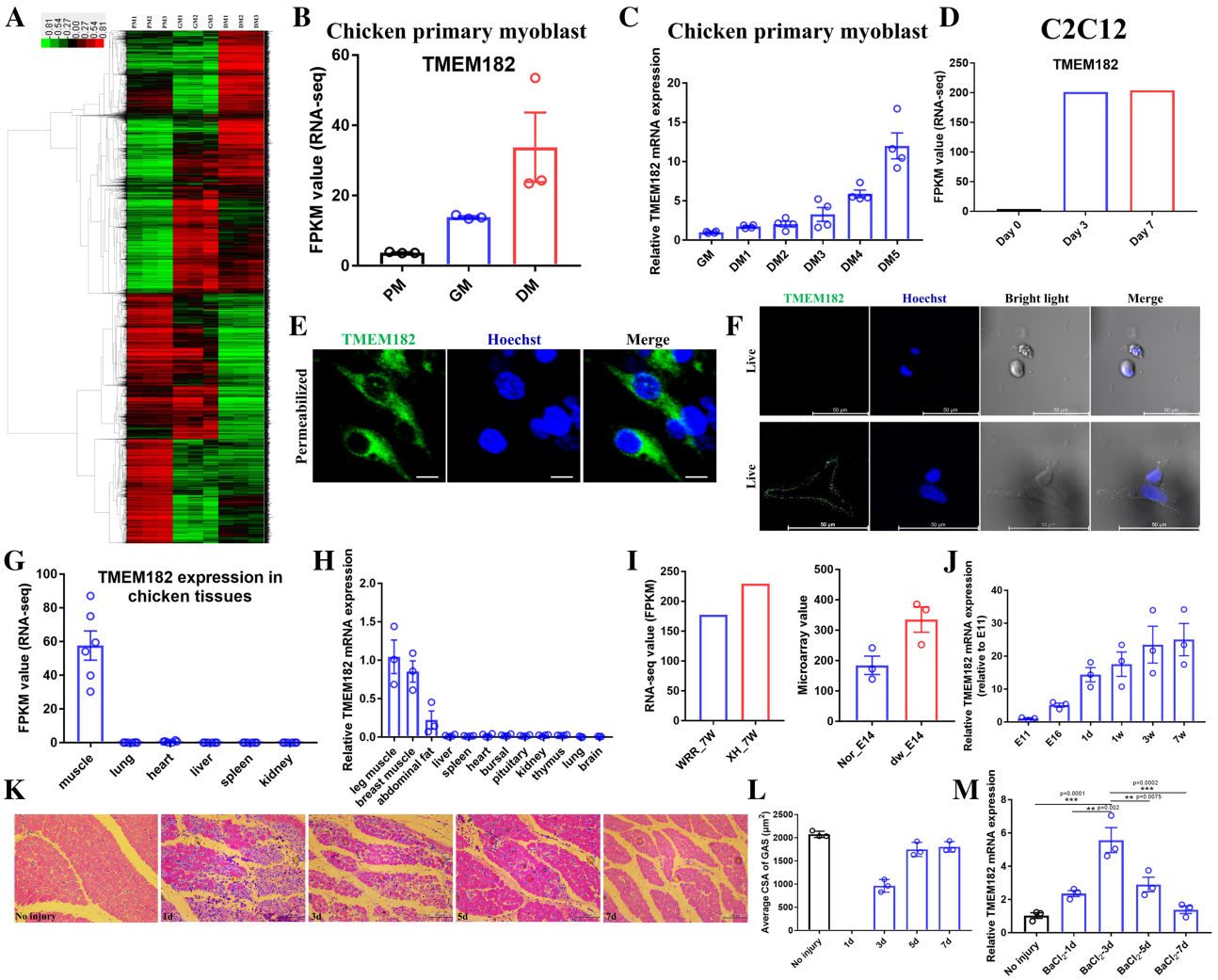

Figure 1 *In vitro* and *in vivo* characterization of *TMEM182* expression in skeletal muscle. *(A)* Hierarchical clustering of differentially expressed genes (DEGs) between chicken PM (primary myoblasts), GM (growing myoblasts), and DM (differentiated myotubes). *(B) TMEM182* mRNA expression in PM, GM, and DM in chickens [n = 3 cultures; mean ± standard error of the mean (SEM)]. *(C)* Quantitative real-time polymerase chain reaction (qPCR) validation of *TMEM182* mRNA expression during chicken primary myoblast differentiation (n = 4 cultures; mean ± SEM). *(D) TMEM182* mRNA expression during C2C12 myoblast differentiation (n = 2 cultures). Data from GSE84158. *(E)* Chicken primary myoblasts were fixed, permeabilized and stained with TMEM182 antibody (green). Hoechst (blue) to show the cell nuclei. Scale bar, 20 μm. *(F)* Freshly isolated chicken primary myoblast (upper) and fused chicken myoblasts (lower) were stained with TMEM182 antibody on ice. After TMEM182 staining (green), cells were then fixed, permeabilized and stained with Hoechst (nuclei, blue) to illustrate cell membrane localization of TMEM182. Scale bar, 50 μm. *(G) TMEM182* mRNA expression in six different chicken tissues (n = 6 chickens; mean ± SEM). Data from GSE93855. *(H)* qPCR validation of *TMEM182* expression in different chicken tissues ($n \geq 3$ chickens; mean ± SEM). *(I) TMEM182* mRNA expression in skeletal muscle from chicken of different breeds. WRR_7W represents white recessive rock chickens at 7 weeks of age, XH_7W represents Xinghua chickens at 7 weeks of age (n = 1, a pooled sample from 3 chickens). Nor_E14 represents normal white recessive rock chickens at embryonic Day 14, dw_E14 represented sex-linked dwarf WRR chicken at embryo Day 14 (n = 3 chickens; mean ± SEM). *(J) TMEM182* mRNA expression during chicken growth (n = 3 chickens; mean ± SEM). *(K)* Representative photographs of haematoxylin and eosin (H&E) staining of chicken gastrocnemius muscle (GAS) at Days 0, 1, 3, 5, and 7 after injury. Scale bar, 100 μm. *(L)* Average cross section area (CSA) of GAS during muscle injury and regeneration (n = 3 chickens; mean ± SEM). *(M) TMEM182* mRNA expression during chicken muscle regeneration (n = 3 chickens; mean ± SEM; one-way analysis of variance (ANOVA) with Tukey's multiple comparison test). The GAS was used to measure mRNA expression. $^{*}P < 0.05$, $^{**}P < 0.01$, $^{***}P < 0.001$.

(*Figure* 1I).[16,17] *TMEM182* expression was gradually up-regulated in skeletal muscle from the embryo stage to adulthood (*Figure* 1J). During skeletal muscle regeneration in chickens (*Figure* 1K), the expression of *TMEM182* was up-regulated at 1 and 3 days after injury and gradually decreased thereafter (*Figure* 1L). From the above results, we deduced that *TMEM182* might be involved in the regulation of myogenesis.

MyoD1 directly binds to an E-box located in the TMEM182 promoter and activates its expression

To explore the regulation of *TMEM182* transcription, we conducted luciferase assays with five reporter constructs containing different fragments of the *TMEM182* promoter (the region between bp − 2527 and +0). Deletion of the region between bp − 548 and +0 bp led to a significant decrease in luciferase activity (*Figure* 2A). Interestingly, two potential E-box sequences exist in the R1 region (*Figure* 2B). E-box 1 is a conserved but non-canonical E-box (*Figure* S5), whereas E-box 2 is a canonical E-box that is not conserved among vertebrates. Deletion of E-box 1 led to a significant decrease in luciferase activity, but E-box 2 deletion did not have any significant effect (*Figure* 2C), suggesting that the conserved E-box 1 is vital for *TMEM182* expression. E-box motifs are potential binding sites for MyoD1, a transcription factor that controls the expression of many muscle-related genes.[18] We overexpressed *MyoD1* and found a significant increase in the luciferase activity of reporter R1 but no significant effect on the mutated E-box 1 reporter (*Figure* 2D). Additionally, *MyoD1* overexpression increased *TMEM182* mRNA expression in chicken primary myoblasts (*Figure* 2E), while inhibition of *MyoD1* was accompanied by decreased *TMEM182* expression (*Figure* 2F). Finally, the results of the ChIP-qPCR assay validated that MyoD1 bound to the promoter region containing E-box 1 (*Figure* 2G). Notably, MyoD1 binding increased from differentiation day (DM) 0 to DM4 (*Figure* 2G). Taken together, these data indicated that MyoD1 directly binds a conserved E-box in the *TMEM182* promoter and induces *TMEM182* transcription during myoblast differentiation.

TMEM182 inhibits myotube formation and skeletal muscle regeneration

To determine the function of *TMEM182* in skeletal muscle cells, we constructed a *TMEM182* overexpression vector and synthesized a siRNA sequence specifically targeting *TMEM182*. *TMEM182* was successfully overexpressed and down-regulated in chicken primary myoblasts (*Figure* S6). Regarding myoblast differentiation and fusion, overexpression of *TMEM182* inhibited the expression of myogenic marker genes, such as *MyoG*, *MyHC*, and *Myomaker*, but did not affect the expression of *MyoD1* (*Figure* 3A). *TMEM182* knockdown had the opposite effects (*Figure* 3B). Then, we used myosin immunofluorescence staining to analyse the function of *TMEM182* in the regulation of myotube formation and myoblast fusion. *TMEM182* overexpression repressed myotube formation and decreased the proportion of myotubes with more than five nuclei (*Figure* 3C–3E), while *TMEM182* knockdown promoted myotube formation and increased the proportion of myotubes with more than five nuclei (*Figure* 3F–3H). These results suggested that *TMEM182* inhibits myoblast differentiation and fusion.

To investigate the physiological implication of *TMEM182*, we constructed a *TMEM182* lentiviral vector to overexpress this protein in chicken GAS muscle (*Figure* 3I). Overexpression of *TMEM182* induced muscle atrophy with a significant reduction in muscle fibre diameter (*Figure* 3J–3K). Next, we investigated the function of *TMEM182* during skeletal muscle regeneration. We overexpressed *TMEM182* after injuring chicken skeletal muscle via injection of $BaCl_2$. H&E staining of muscle sections at different times after injury showed that at 7 and 9 days after $BaCl_2$ injection, most of the inflammatory myofibres in the control chicks had been replaced by newly formed myofibres with a complete and clear structure, but more necrotic myofibres and inflammatory cells remained in the *TMEM182*-overexpressing chicks (*Figure* 3L–3M). Additionally, we examined the expression of embryonic *MyHC* (*eMyHC*), adult *MyHC* (*MyHC*), and *Desmin*, which are markers of muscle regeneration, on different days after $BaCl_2$ injection. *TMEM182* expression was significantly up-regulated in injured skeletal muscle (*Figure* 3N), and the expression of adult *MyHC* in muscle was significantly higher in the control group than in the *TMEM182* overexpression group (*Figure* 3O), suggesting a greater number of regenerated muscle fibres in the control group. At 3 and 5 days, regenerating myofibres in control muscle exhibited higher *eMyHC* and *Desmin* expression levels than those in *TMEM182* overexpressing muscle (*Figure* 3P–3Q), indicating that the muscle regeneration programme is more active in control muscle. These results indicated that muscle regeneration in *TMEM182* overexpressing muscle lags behind that in control muscle.

TMEM182 KO in mice significantly increases muscle mass and muscle fibre size

TMEM182 is a conserved gene in all vertebrates, and the amino acid sequence of the TMEM182 protein is conserved among vertebrates (*Figure* S7). To better understand the role of *TMEM182* in muscle development at the individual animal level, we generated *TMEM182*-KO mice using CRISPR/Cas9-mediated genome editing. A 2517 bp genomic region encompassing exons 2 and 3 of *TMEM182* was deleted, and different genotypes were identified by PCR and sequencing (*Figures* 4A and S8). *TMEM182*-KO mice were healthy and were larger than WT mice (*Figure* 4B). The western blot results showed that *TMEM182* expression was barely detectable in skeletal muscle of the KO mice (*Figure* 4B). Notably, the *TMEM182*-KO mice were heavier than the WT mice (*Figure* 4C–4D). Considering that *TMEM182* plays an inhibitory role in muscle cell development, we compared the skeletal muscle weight, skeletal muscle fibre number, and skeletal muscle fibre diameter between KO and WT mice. The GAS,

DOI: 10.1002/jcsm.12767

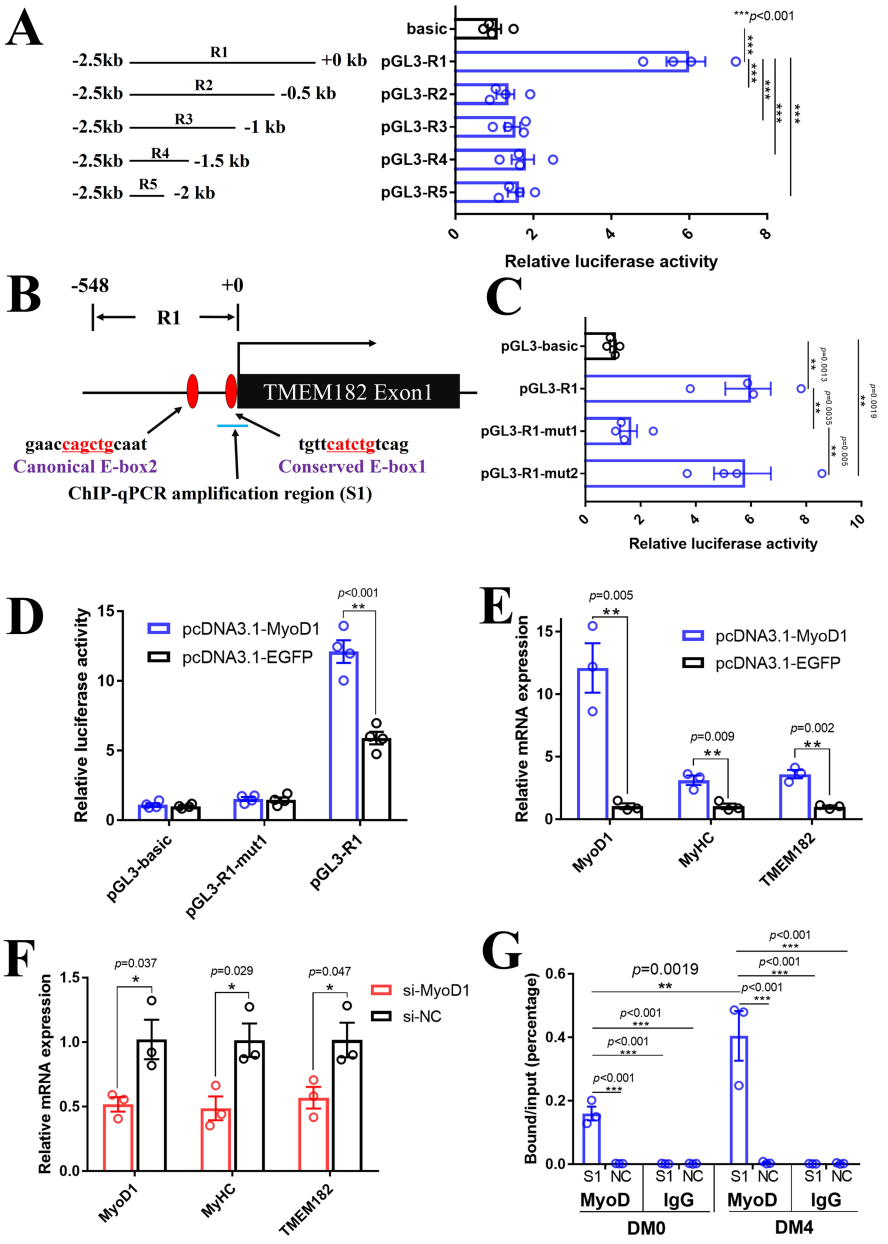

Figure 2 MyoD1 directly binds to an E-box in the *TMEM182* promoter and activates its expression. *(A)* Luciferase assays after transfecting five reporter constructs into chicken primary myoblasts. Deletion of the region between +0 bp and −500 bp significantly reduced luciferase activity. Left: schematic of the five reporter constructs used for luciferase assays. Right: Chicken primary myoblasts were transfected with *TMEM182* reporter constructs containing various fragments, and reporter luciferase activity was measured (n = 4 cultures; mean ± SEM; one-way ANOVA with Tukey's multiple comparison test). *(B)* Location of E-box 1 and E-box 2 in the chicken *TMEM182* gene promoter. *(C)* Relative luciferase activity of reporters harbouring mutant E-box 1 (mut1) or E-box 2 (mut2). This assay was performed in chicken myoblasts (n = 4 cultures; mean ± SEM; one-way ANOVA with Tukey's multiple comparison test). *(D) MyoD1* overexpression promotes the luciferase activity of a reporter containing the *TMEM182* promoter in chicken myoblasts (n = 4 cultures; mean ± SEM; two-sided Student's t-test). *(E)* qPCR results showed that *MyoD1* overexpression promoted *TMEM182* mRNA expression in chicken myoblasts (n = 3 cultures; mean ± SEM; two-sided Student's t-test). *(F)* qPCR results showed that *MyoD1* knockdown by si-MyoD1 repressed *TMEM182* mRNA expression in chicken myoblasts (n = 3 cultures; mean ± SEM; two-sided Student's t-test). *(G)* Chromatin immunoprecipitation (ChIP)-qPCR analysis using anti-MyoD1 or chicken IgG showed that MyoD1 could bind to the S1 region (as indicated in B) of the chicken *TMEM182* gene in chicken myoblasts at day 0 of differentiation medium (DM0) and DM4 (n = 3 cultures; mean ± SEM; two-way ANOVA with Tukey's multiple comparison test). A region of the *glyceraldehyde-3-phosphate dehydrogenase* (*GAPDH*) gene was amplified as a negative control to verify the specificity of the enrichment [shown as negative control (NC)]. $^{*}P < 0.05$, $^{**}P < 0.01$, $^{***}P < 0.001$.

DOI: 10.1002/jcsm.12767

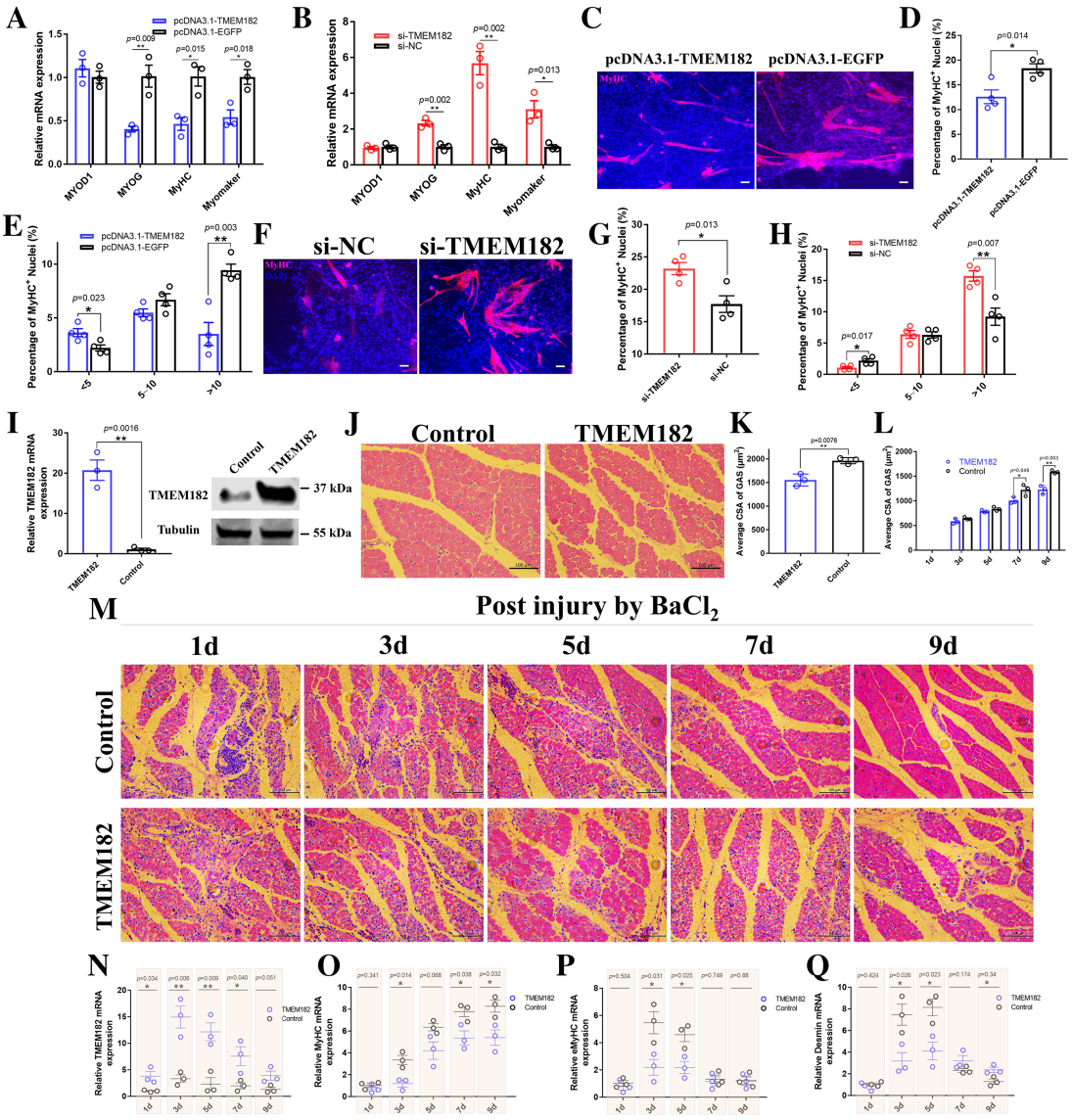

Figure 3 *TMEM182* inhibits myotube formation and skeletal muscle regeneration. *(A)* Relative mRNA expression of muscle differentiation and fusion marker genes in chicken myoblasts overexpressing *TMEM182* (n = 3 cultures; mean ± SEM; two-sided Student's t-test). *(B)* Relative mRNA expression of muscle differentiation and fusion marker genes in chicken myoblasts with *TMEM182* knockdown (n = 3 cultures; mean ± SEM; two-sided Student's t-test). *(C)* MyHC staining of cells at 72 h after *TMEM182* overexpression in chicken myoblasts. Fused myotubes were positive for MyHC (red), cell nuclei were positive for DAPI (blue). Bar, 50 μm. *(D)* Fusion rate at 72 h in chicken myoblasts overexpressing *TMEM182* (n = 4 cultures; mean ± SEM; two-sided Student's t-test). *(E)* Distribution of MyHC positive nuclei at 72 h in chicken myoblasts overexpressing *TMEM182* (n = 4 cultures; mean ± SEM; two-sided Student's t-test). *(F)* MyHC staining of cells at 72 h after *TMEM182* knockdown in chicken myoblasts. Fused myotubes were positive for MyHC (red), cell nuclei were positive for DAPI (blue). Bar, 50 μm. *(G)* Fusion rate at 72 h in chicken myoblasts with *TMEM182* knockdown (n = 4 cultures; mean ± SEM; two-sided Student's t-test). *(H)* Distribution of MyHC positive nuclei at 72 h in chicken myoblasts with *TMEM182* knockdown (n = 4 cultures; mean ± SEM; two-sided Student's t-test). *(I) TMEM182* levels after overexpression in chicken gastrocnemius (Gas) muscle (n = 3 chickens; mean ± SEM; two-sided Student's t-test). *(J)* Representative photographs of H&E staining of gas muscles from chickens overexpressing *TMEM182*. Bar, 100 μm. *(K)* Statistical analysis of the muscle fibre CSA in Gas muscles from chickens overexpressing *TMEM182* (n = 3 chickens; mean ± SEM; two-sided Student's t-test). *(L)* Quantification of CSA of chicken Gas muscle at Days 3, 5, 7, and 9 after injury. *EGFP* lentivirus was used as the control (n = 3 chickens; mean ± SEM; two-sided Student's t-test). *(M)* Representative photographs of H&E staining of chicken Gas muscle at Days 1, 3, 5, 7, and 9 after injury. *EGFP* lentivirus was used as the control. Bar, 100 μm. *(N) TMEM182* mRNA expression at different stages of muscle regeneration in chickens transfected with *TMEM182* or control. *(O)* The mRNA expression of adult *MyHC*, a marker gene indicating the degree of muscle recovery, at different stages of muscle regeneration in chickens transfected with *TMEM182* or control. *(P)* The mRNA expression of *eMyHC*, a marker gene indicating the activity of muscle regeneration, at different stages of muscle regeneration in chickens transfected with *TMEM182* and control. *(Q)* The mRNA expression of *Desmin*, a marker gene indicating the activity of muscle regeneration, at different stages of muscle regeneration in chickens transfected with *TMEM182* and control. For *(N)–(Q)*, the results are shown as the mean ± SEM (n = 3 chickens; mean ± SEM; two-sided Student's t-test).

DOI: 10.1002/jcsm.12767

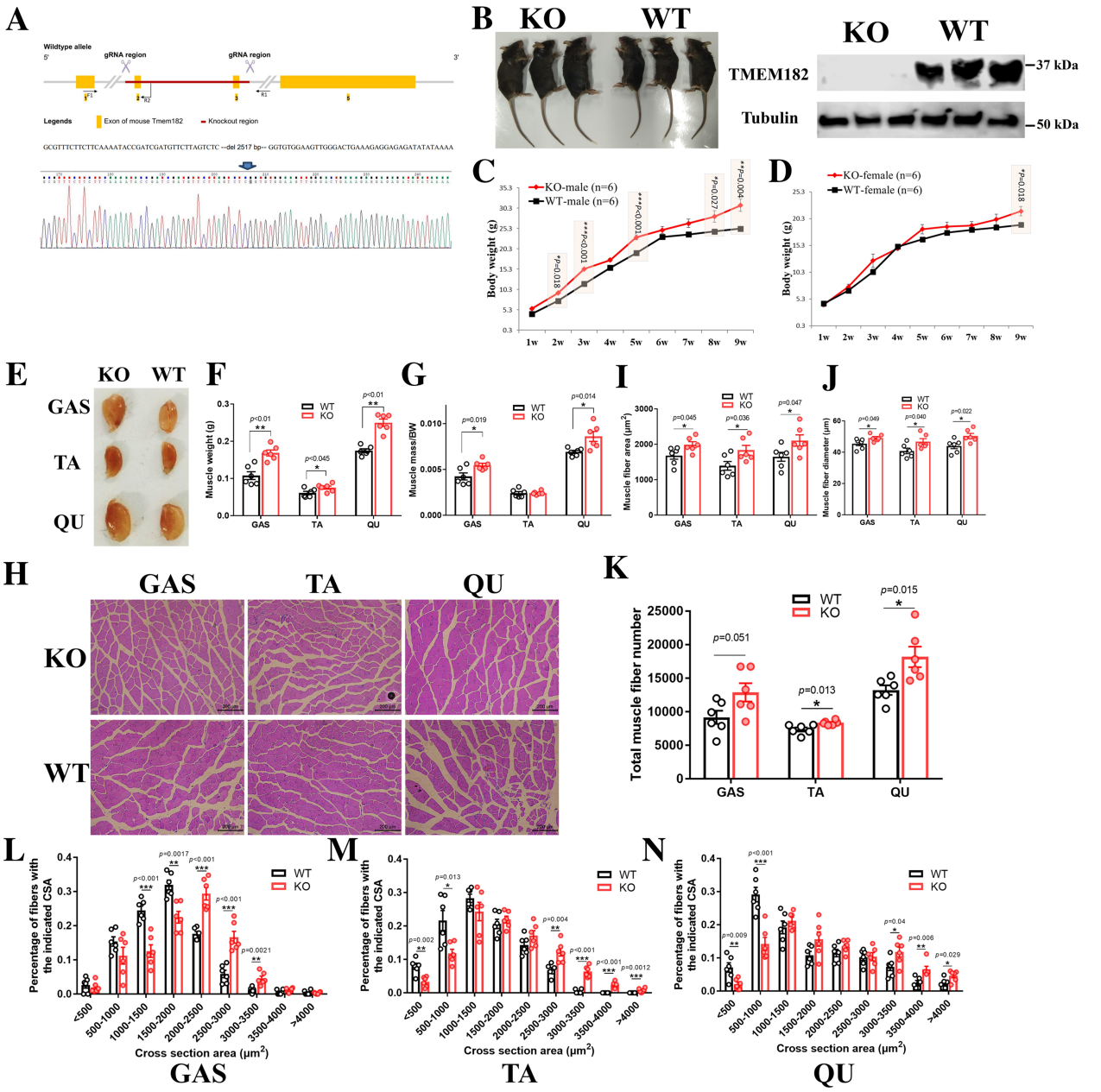

Figure 4 *TMEM182* KO in mice significantly increases muscle mass, muscle fibre size, and muscle fibre number. *(A)* Location of the knockout (KO) region in the mouse *TMEM182* gene. *(B) TMEM182* knockout increased mouse body size (left) and eliminated TMEM182 protein expression (right). *(C)* Growth curves of *TMEM182* KO and wild-type (WT) mice showing that *TMEM182* knockout increased the body weight of male mice. *(D)* Growth curves of *TMEM182* KO and WT mice showing that *TMEM182* knockout increased the body weight of female mice. *(E)* Representative photographs of skeletal muscles indicating that *TMEM182* KO increased mouse muscle size. *(F)* Statistical analysis of muscle weight indicating that *TMEM182* KO increased mouse muscle weight. *(G)* The Gas, tibialis anterior (TA), and quadriceps (QU) muscles were significantly heavier in *TMEM182* KO mice than in WT mice. All data were normalized to body weight (mg/g). *(H)* Representative photographs of H&E staining of Gas, TA, and Qu muscles from 9-week-old *TMEM182*-KO and WT mice. Bar, 200 μm. *(I)* Statistical analysis indicating that *TMEM182* KO increased mouse muscle fibre area. *(J)* Statistical analysis indicating that *TMEM182* KO increased mouse muscle fibre diameter. *(K)* Statistical analysis indicating that *TMEM182* KO increased mouse total muscle fibre number. *(L–N)* Comparison of the percentage of muscle fibres with the indicated cross-sectional area in *TMEM182* KO mice and WT mice. For *(C), (D), (F)–(J), (K)–(N)*, the results are shown as the mean ± SEM (*n* = 6 mice; two-sided Student's *t*-test).

tibialis anterior, and quadriceps muscle weights were significantly higher in the *TMEM182*-KO mice than in the WT mice (*Figure* 4E–4F). Importantly, the ratio of muscle to body weight in the *TMEM182*-KO mice was also significantly higher than that in the WT mice (*Figure* 4G). Next, we used H&E staining to assess changes in muscle fibre number and size

in the *TMEM182*-KO mice (*Figure* 4H). The mean CSA and diameter of individual myofibres were significantly larger in the TMEM182-KO mice than in the WT mice (*Figure* 4I–4J), and these KO mice had more total muscle fibres than the WT mice (*Figure* 4K). The results also showed that the *TMEM182*-KO mice had a significantly higher proportion of larger myofibres (*Figure* 4L–4N). Finally, the RNA-seq data (*Table* S4) for GAS muscle from KO and WT mice showed that the DEGs (*Table* S5) were enriched in pathways involved in skeletal muscle hypertrophy and growth, such as phosphatidylinositol 3-kinase-Akt (PI3K-Akt) signalling, insulin signalling, extracellular matrix (ECM)-receptor interaction, focal adhesion, and Toll-like receptor signalling pathways (*Figure* S9A). GSEA of the RNA-seq data also demonstrated that loss of *TMEM182* led to positive enrichment of muscle hypertrophy and muscle tissue development (*Figure* S9B–S9C). Thus, these results indicate that *TMEM182* KO in mice significantly increases muscle mass and muscle fibre size.

TMEM182 KO increases myotube formation and accelerates muscle regeneration

To further confirm the roles of *TMEM182* in myoblast differentiation and fusion, we isolated primary skeletal muscle myoblasts from the leg muscles of WT and *TMEM182*-KO mice. *TMEM182* KO in primary myoblasts significantly promoted the expression of *MyoG*, *MyHC*, and *Myomaker*, but did not significantly affect the expression of *MyoD1* (*Figure* 5A). Additionally, myosin immunofluorescence staining showed that *TMEM182* KO significantly increased the number of myotubes and increased the myoblast fusion rate, as determined by the greater number of nuclei in each myotube (*Figure* 5B–5D). These results indicated that *TMEM182* KO promotes myoblast differentiation.

To further understand the role of *TMEM182* in muscle regeneration, we used CTX to induce muscle injury in WT and *TMEM182*-KO mice. H&E staining showed that at 11 and 15 days after CTX injection, most of the inflammatory myofibres in the *TMEM182*-KO mice had been replaced by newly formed myofibres with complete and clear structures, whereas many inflammatory cells and necrotic myofibres remained in the WT mice (*Figures* 5E and S10A). At 19 days after CTX injection, muscle regeneration and repair were complete in the *TMEM182*-KO mice, whereas newly formed myofibres with central nuclei were still present in the WT mice (*Figures* 5E–5F and S10A–S10B). Additionally, the expression levels of *eMyHC* and *Desmin*, markers of muscle regeneration, were higher in the KO mice than in the WT mice at early regeneration stages (*Figures* 5G–5H and S10C–S10D). However, at 15 and 19 days, the WT mice had higher *eMyHC* and *Desmin* expression level than the *TMEM182*-KO mice (*Figures* 5G–5H and S10C–S10D). These results suggested that *TMEM182* KO accelerates muscle regeneration.

TMEM182 directly interacts with ITGB1

To further understand the mechanism by which *TMEM182* inhibits myogenesis, we used co-immunoprecipitation and mass spectrometry to screen the proteins bound to TMEM182 in chicken primary myoblasts. The mass spectrometry analysis results revealed that ITGB1, an essential membrane receptor involved in cell adhesion and muscle development, is a potential binding protein of TMEM182 (*Table* S2). To confirm the TMEM182-ITGB1 association, we immunoprecipitated TMEM182 in myoblasts overexpressing TMEM182 or EGFP and found that both TMEM182 and ITGB1 were present in the precipitate (*Figure* 6A). Next, we immunoprecipitated endogenous ITGB1 in the lysate of dissected chicken gastrocnemius muscle and found that the precipitate contained not only TMEM182 and ITGB1 but also a common ITGB1 partner, ITGA7 (*Figure* 6B). By using a GST pulldown assay, we further validated the interaction between TMEM182 and ITGB1 (*Figure* 6C).

ITGB1 is a conserved cell surface receptor with multiple functional domains. By using the Pfam database, we predicted several functional domains in the chicken ITGB1 protein (*Figure* 6D). Then, a series of ITGB1 domains were constructed, and their ability to interact with TMEM182 was evaluated. The GST pull-down results showed that the peptide containing the hybrid domain (aa 387–470) directly interacted with TMEM182 (*Figure* 6E), indicating that the hybrid domain of ITGB1 is responsible for its binding to TMEM182. Transmembrane proteins have transmembrane--spanning regions that pass through the lipid bilayer of the cell membranes; the TMEM182 protein was predicted by Phyre2 to contain four transmembrane spans with both the N-terminus and C-terminus in the intracellular space (*Figure* 6F). Next, to search for the binding domain of TMEM182 to ITGB1, we constructed two flag-tagged TMEM182 mutant proteins—one with deletion of the large extracellular loop (Δ30–113) and one with deletion of the small extracellular loop (Δ174–196). The GST pull down results showed that deletion of the large extracellular loop abolished the ability of TMEM182 to bind to ITGB1, whereas deletion of the small extracellular loop had no effect on the binding ability (*Figure* 6G). Notably, we found that the aa 52–62 region within the predicted large extracellular loop of TMEM182 was highly conserved among vertebrates (*Figure* S11). Deletion of these 11 conserved amino acids abolished the ability of TMEM182 to bind to ITGB1, whereas deletion of the adjacent region (aa 75–110) had no effect on the binding ability (*Figure* 6H). These results indicated that TMEM182 directly interacts with ITGB1.

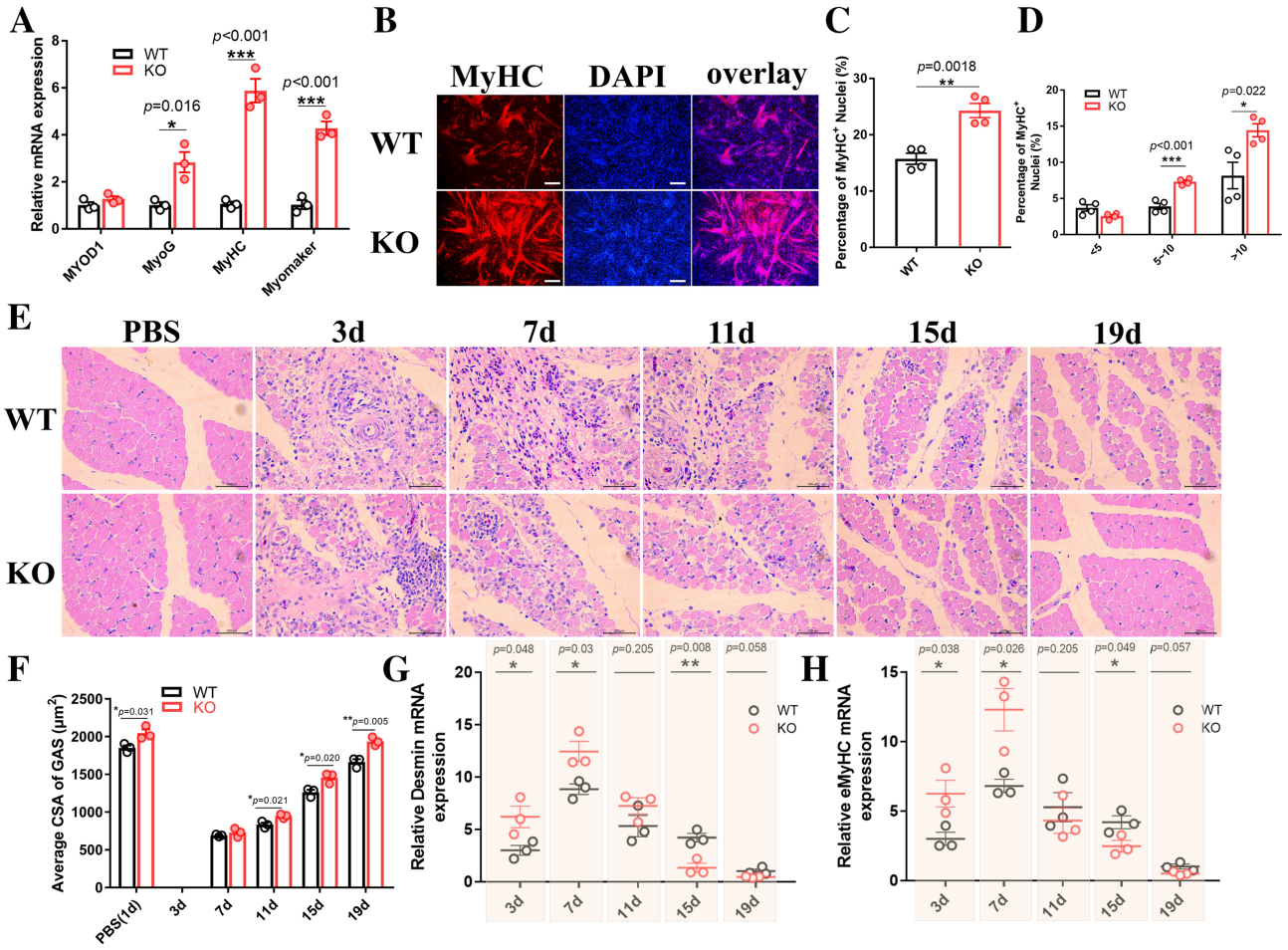

Figure 5 *TMEM182* KO increases myotube formation and accelerates muscle regeneration. *(A)* Relative mRNA expression of muscle differentiation and fusion marker genes indicating that *TMEM182* knockout increased *MyoG*, *MyHC*, and *Myomaker* mRNA expression in mice (n = 3 cultures; mean ± SEM; two-sided Student's t-test). *(B)* MyHC staining of the indicated mouse primary myoblasts at 72 h after the induction of differentiation. Fused myotubes were positive for MyHC (red), cell nuclei were positive for DAPI (blue). Bar, 100 μm. *(C)* Fusion rate of the indicated mouse primary myoblasts at 72 h after the induction of differentiation (n = 4 cultures; mean ± SEM; two-sided Student's t-test). *(D)* Distribution of MyHC positive nuclei in *TMEM182*-KO mouse myotubes and WT mouse myotubes (n = 4 cultures; mean ± SEM; two-sided Student's t-test). *(E)* Representative photographs of H&E staining of Gas muscle at Days 3, 7, 11, 15, and 19 after cardiotoxin (CTX) injury showing that muscle damage repair is completed faster in *TMEM182*-KO mice than in WT mice. Bar, 200 μm. *(F)* Average CSA of GAS muscle during *TMEM182*-KO mice and WT mice muscle regeneration (n = 3 mice; mean ± SEM; two-sided Student's t-test). *(G)* The mRNA expression of *Desmin*, a marker gene indicating the activity of muscle regeneration, at different stages of muscle regeneration in *TMEM182*-KO mice and WT mice (n = 3 mice; mean ± SEM; two-sided Student's t-test). *(H)* The mRNA expression of *eMyHC*, a marker gene indicating the activity of muscle regeneration, at different stages of muscle regeneration in *TMEM182*-KO mice and WT mice (n = 3 mice; mean ± SEM; two-sided Student's t-test).

Regulation of myoblast differentiation by TMEM182 depends on ITGB1

ITGB1 plays an essential role in myoblast differentiation and fusion; thus, we sought to determine whether *ITGB1* is involved in the regulatory function of *TMEM182* in myoblast differentiation. Either *TMEM182* overexpression or *ITGB1* knockdown decreased the expression of myogenic marker genes (*Figures* 7A and S12). Deletion of the conserved TMEM182 domain (aa 52–62), which impaired the interaction of TMEM182 with the hybrid domain of ITGB1, abolished the inhibitory effect of *TMEM182* on myogenic differentiation (*Figure* 7A). Interestingly, *TMEM182* overexpression did not further inhibit myogenic differentiation in *ITGB1* knockdown cells compared with control cells (*Figure* 7A). The myosin immunofluorescence staining results also demonstrated that *TMEM182* overexpression did not inhibit myoblast fusion and multinucleated myotube formation in *ITGB1* knockdown cells compared with control cells (*Figure* 7B–7D). On the other hand, the negative effect of *TMEM182* on myogenic differentiation was rescued by *ITGB1* overexpression (*Figure* 7E). ITGB1

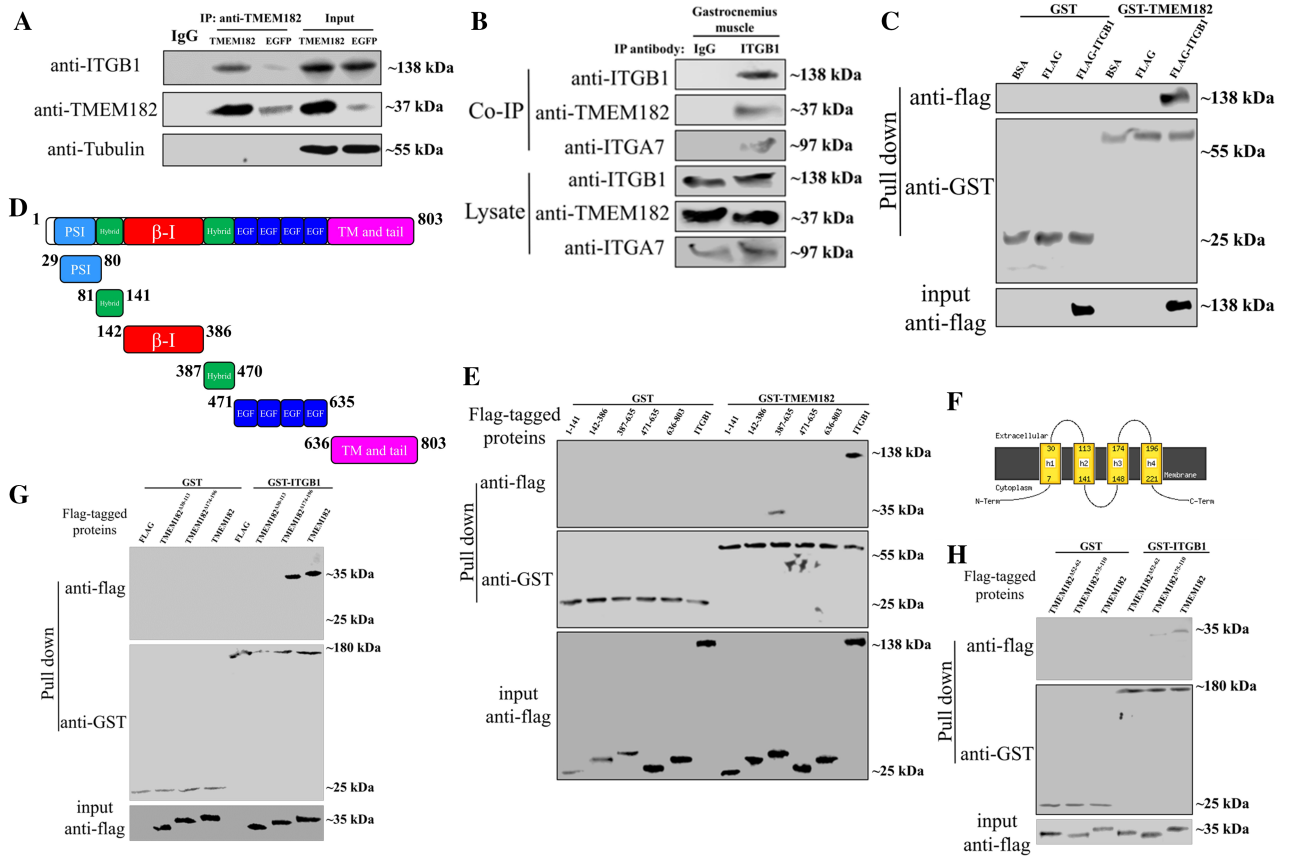

Figure 6 TMEM182 directly interacts with ITGB1. *(A)* Lysates of chicken primary myoblasts overexpressing *TMEM182* or *EGFP* control were immunoprecipitated with TMEM182 antibody and then Western blotted with anti-β1 integrin (anti-ITGB1), anti-TMEM182, and anti-tubulin. *(B)* Lysates of chicken gastrocnemius muscle were immunoprecipitated with ITGB1 antibody and then Western blotted with anti-ITGB1, anti-TMEM182, and anti-ITGA7. *(C)* Flag vector or FLAG-ITGB1 was transfected into chicken primary myoblasts and immunoprecipitated with anti-FLAG-agarose beads followed by eluting with FLAG peptide. GST-TMEM182 or control glutathione-S-transferase (GST) protein was incubated with purified FLAG-ITGB1, FLAG peptide, or bovine serum albumin for pull-down assay and then Western blotted with FLAG antibody. The amounts of GST and GST-TMEM182 used in this experiment were indicated by immunoblotting with anti-GST antibody (middle panel). *(D)* Schematic diagram of chicken TMEM182 and its putative domains. *(E)* FLAG-tagged ITGB1 or domain constructs as shown in *(D)* was transfected into chicken myoblast and purified by using anti-FLAG-agarose beads (bottom panel). GST or GST-TMEM182 fusion protein was incubated with purified FLAG-tagged proteins for direct pull-down assay (top panel). *(F)* The predicted transmembrane helices of chicken TMEM182 protein. *(G–H)* FLAG-tagged TMEM182 or mutant constructs was transfected into chicken myoblast and purified by using anti-FLAG-agarose beads (bottom panel). GST or GST-ITGB1 fusion protein was incubated with purified FLAG-tagged proteins for direct pull-down assay (top panel).

overexpression induced higher expression of myogenic marker genes in *TMEM182*-KO myoblasts compared with WT myoblasts (*Figure* 7F). These results suggest that TMEM182 restricts ITGB1 function during myogenesis and that the regulation of myoblast differentiation by *TMEM182* depends on *ITGB1*.

TMEM182 affects the ITGB1-laminin interaction and inhibits ITGB1 mediated intracellular signalling during myogenesis

Laminins are essential and biologically active components of the ECM, influencing cell differentiation, migration, and adhesion. ITGB1 is a laminin receptor in skeletal muscle. The ITGB1-laminin interaction regulates myoblast differentiation, migration, and adhesion.[19,20] To test whether the binding of *TMEM182* to ITGB1 affects the interaction between ITGB1 and laminin, we immunoprecipitated ITGB1 in myoblasts overexpressing *TMEM182* or *EGFP* as the control. We found that *TMEM182* overexpression significantly reduced the amount of laminin bound to ITGB1 (*Figure* 8A) and that KO of *TMEM182* in mice increased the amount of laminin bound to ITGB1 (*Figure* 8B). CTX induced muscle regeneration accompanied by increased ITGB1 expression, and *TMEM182* KO increased the interaction between ITGB1 and laminin during muscle regeneration (*Figure* 8B).

Because the ITGB1-laminin interaction is essential for myoblast migration and adhesion, we speculated that the binding of TMEM182 to ITGB1 affects myoblast migration and

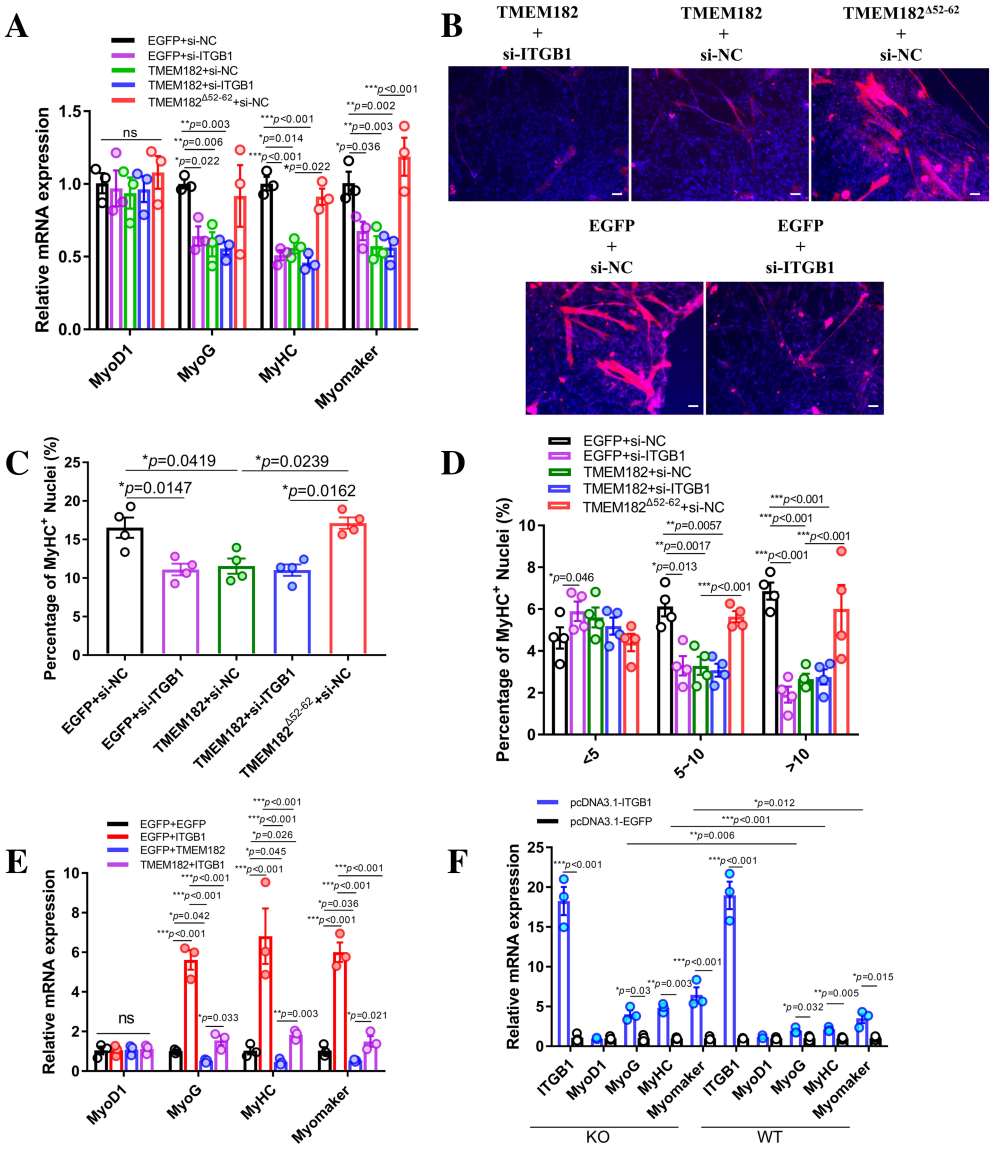

Figure 7 Regulation of myoblast differentiation by TMEM182 depends on ITGB1. *(A) TMEM182*, mutated *TMEM182* and *EGFP* overexpression vector were transfected into *ITGB1* knockdown or control chicken myoblasts, and the relative mRNA expression of *MyoD1*, *MyoG*, *MyHC*, and *Myomaker* was analysed (n = 3 cultures; mean ± SEM; one-way ANOVA with Tukey's multiple comparison test). *(B–D) TMEM182*, mutated *TMEM182* and *EGFP* overexpression vector were transfected into *ITGB1* knockdown or control chicken myoblasts, and myotube formation and the fusion index were analysed (n = 4 cultures; mean ± SEM; one-way ANOVA with Tukey's multiple comparison test). Fused myotubes were positive for MyHC (red), cell nuclei were positive for DAPI (blue). Bar, 50 μm. *(E) ITGB1* and *EGFP* overexpression vector were transfected into *TMEM182* overexpressing or control chicken myoblasts, and the relative mRNA expression of *MyoD1*, *MyoG*, *MyHC*, and *Myomaker* was analysed (n = 3 cultures; mean ± SEM; one-way ANOVA with Tukey's multiple comparison test). *(F) ITGB1* overexpression vector was transfected into *TMEM182*-KO mice primary myoblast or WT mice primary myoblast, and the relative mRNA expression of *ITGB1*, *MyoD1*, *MyoG*, *MyHC*, and *Myomaker* was analysed (n = 3 cultures; mean ± SEM; two-way ANOVA with Tukey's multiple comparison test).

adhesion. By using a wound healing assay, we found that *TMEM182* overexpression slowed cell migration, whereas mutation of the ITGB1 binding domain in TMEM182 abolished the inhibitory effect of TMEM182 on myoblast migration (*Figure* 8C–8D). The Transwell assay results further validated that *TMEM182* inhibits myoblast migration, and this inhibitory effect was found to be abolished when the ITGB1 binding domain in TMEM182 was mutated (*Figure* 8E–8F). Additionally, the percentage of adherent myoblasts among *TMEM182*-overexpressing cells was significantly reduced (*Figure* 8G), indicating that *TMEM182* inhibits myoblast adhesion. However, the inhibitory effects of *TMEM182* on myoblast migration and adhesion were rescued by *ITGB1* transfection (*Figure* 8H–8J), indicating the essential role of

DOI: 10.1002/jcsm.12767

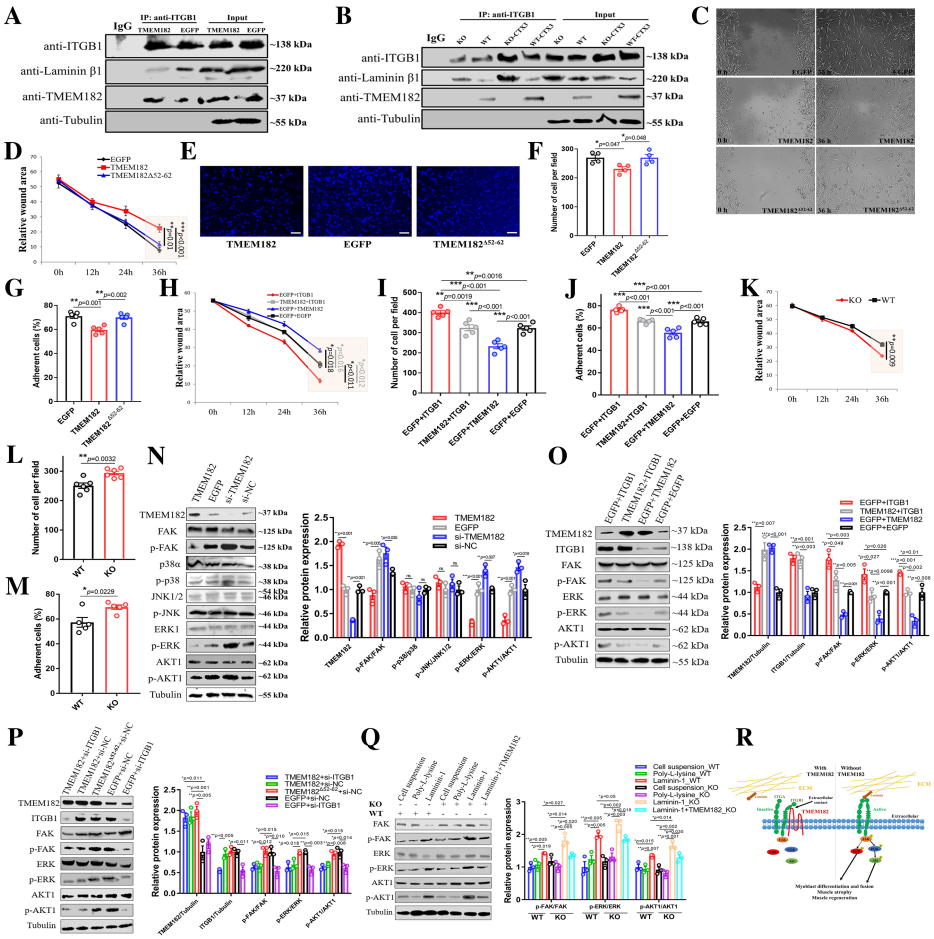

Figure 8 *TMEM182* affects ITGB1-Laminin interaction and inhibits ITGB1 mediated intracellular signalling during myogenesis. *(A)* Lysates of chicken primary myoblasts overexpressing *TMEM182* or *EGFP* control were immunoprecipitated with ITGB1 antibody and then Western blotted with anti-ITGB1, anti-Laminin β1, anti-TMEM182, and anti-tubulin. *(B)* Lysates of hindlimb muscle from *TMEM182*-KO mice, WT mice, *TMEM182*-KO mice 3 days after CTX injured, and WT mice *TMEM182*-KO mice were immunoprecipitated with ITGB1 antibody and then Western blotted with anti-ITGB1, anti-Laminin β1, anti-TMEM182, and anti-tubulin. *(C)* Representative figures of the classic scratch assay for chicken myoblasts transfected with *TMEM182*, mutated *TMEM182*, or *EGFP*. *(D)* Statistical analysis of the relative wound area in the classic scratch assay for chicken myoblasts overexpressing *TMEM182*, mutated *TMEM182*, or *EGFP* (n = 3 cultures; mean ± SEM; one-way ANOVA with Tukey's multiple comparison test). *(E)* Transwell migration assay using chicken myoblasts transfected with pcDNA3.1-TMEM182, pcDNA3.1-TMEM182$^{\Delta 52–62}$ or pcDNA3.1-EGFP. Bar, 100 μm. *(F)* The statistical results of cell number in Transwell migration assay for chicken myoblasts transfected with pcDNA3.1-TMEM182, pcDNA3.1-TMEM182$^{\Delta 52–62}$ or pcDNA3.1-EGFP (n = 4 cultures; mean ± SEM; one-way ANOVA with Tukey's multiple comparison test). *(G)* Chicken myoblasts were transfected with pcDNA3.1-TMEM182, pcDNA3.1-TMEM182$^{\Delta 52–62}$ or pcDNA3.1-EGFP for 24 h in serum-free medium. After washing once in PBS to remove non-adherent cells, the remaining adherent cells were assessed using MTT (3-[4, 5-dimethylthiazol-2-yl]-2, 5 diphenyl tetrazolium bromide) assay (n = 5 cultures; mean ± SEM; one-way ANOVA with Tukey's multiple comparison test). *(H)* Statistical analysis of the relative wound area in the classic scratch assay for chicken myoblasts transfected with indicated vectors (n = 3 cultures; mean ± SEM; one-way ANOVA with Tukey's multiple comparison test). *(I)* The statistical results of cell number in Transwell migration assay for chicken myoblasts transfected with indicated vectors (n = 5 cultures; mean ± SEM; one-way ANOVA with Tukey's multiple comparison test). *(J)* Chicken myoblasts were transfected with indicated vectors for 24 h in serum-free medium. After washing once in PBS to remove non-adherent cells, the remaining adherent cells were assessed using MTT assay (n = 5 cultures; mean ± SEM; one-way ANOVA with Tukey's multiple comparison test). *(K)* Statistical analysis of the relative wound area in the classic scratch assay for *TMEM182*-KO mouse myoblasts and WT mouse myoblasts (n = 3 cultures; mean ± SEM; two-sided Student's t-test). *(L)* The statistical results of cell number in Transwell migration assay for *TMEM182*-KO mouse myoblasts and WT mouse myoblasts (n = 6 cultures; mean ± SEM; two-sided Student's t-test). *(M) TMEM182*-KO mouse myoblasts and WT mouse myoblasts were cultured for 24 h in serum-free medium. After washing once in PBS to remove non-adherent cells, the remaining adherent cells were assessed using MTT assay (n = 6 cultures; mean ± SEM; two-sided Student's t-test). *(N)* Representative immunoblots (left) and quantification (right, n = 3 cultures; mean ± SEM; two-sided Student's t-test) of indicated antibodies in lysates of chicken myoblasts transfected with pcDNA3.1-TMEM182, pcDNA3.1-EGFP, si-TMEM182, and si-NC. *(O–P)* Representative immunoblots (left) and quantification (right, n = 3 cultures; mean ± SEM; two-sided Student's t-test) of indicated antibodies in lysates of chicken myoblasts transfected with indicated overexpression vectors. *(Q)* Representative immunoblots (left) and quantification (right, n = 3 cultures; mean ± SEM; two-way ANOVA with Tukey's multiple comparison test) of indicated antibodies in lysates of WT and *TMEM182*-KO mouse myoblasts. Myoblasts was transfected with or without pcDNA3.1-TMEM182 for 48 h, then the cells were plated on poly-L-lysine or laminin-1 for 1 h. Samples were analysed by SDS–PAGE and immunoblotted with indicated antibodies. *(R)* Proposed mechanistic model of the *TMEM182* in myogenesis and muscle regeneration.

DOI: 10.1002/jcsm.12767

ITGB1 in *TMEM182* function. Furthermore, *TMEM182* KO not only increased the migration of mouse primary myoblasts but also increased myoblast adhesion (*Figure* 8K–8M). Thus, *TMEM182* inhibits myoblast migration and adhesion by binding to ITGB1.

The interaction between ITGB1 and laminin activates ITGB1-mediated intracellular signalling pathways, such as the FAK pathway, mitogen-activated protein kinase pathway, and PI3K-Akt pathway. These ITGB1-mediated downstream pathways have been implicated in myogenesis and skeletal muscle regeneration. As *TMEM182* affects the interaction between ITGB1 and laminin, we investigated whether *TMEM182* regulates ITGB1 mediated signalling pathways during myoblasts differentiation. Overexpression of *TMEM182* reduced the phosphorylation of FAK, extracellular signal-regulated kinase (ERK), and Akt in differentiating myoblasts, whereas knockdown of *TMEM182* enhanced the phosphorylation of these three proteins (*Figure* 8N). *TMEM182* KO also enhanced FAK and Akt phosphorylation in mice (*Figure* S13). However, co-overexpression of *ITGB1* and *TMEM182* rescued the inhibitory effect of TMEM182 on the phosphorylation of FAK, ERK, and Akt (*Figure* 8O). Additionally, deletion of the conserved TMEM182 domain (aa 52–62), which impaired the interaction of TMEM182 with the hybrid domain of ITGB1, abolished the inhibitory effects of TMEM182 on the phosphorylation of FAK, ERK, and Akt (*Figure* 8P). Knockdown of *ITGB1* suppressed the effects of *TMEM182* on the inhibition of FAK, ERK, and Akt protein activation (*Figure* 8P). Furthermore, laminin-stimulated activation of the FAK, ERK, and Akt proteins was enhanced in *TMEM182*-KO myoblasts compared with WT myoblasts, and *TMEM182* transfection diminished the activation of these three proteins in *TMEM182*-KO myoblasts (*Figure* 8Q). Thus, we concluded that TMEM182 interacts with ITGB1 to regulate ITGB1 ligand binding and ITGB1 downstream signalling during myogenesis.

Discussion

In this study, using chickens and mice, which are ideal model animals for myogenesis research, we found that the transmembrane protein *TMEM182* inhibits myogenesis and muscle regeneration. The negative effects of the *TMEM182* protein on myogenesis depend on its interaction with ITGB1. We established that the ITGB1-*TMEM182* protein complex is formed via a direct interaction and likely involves a lateral interaction between the extracellular domains of each protein. Direct extracellular contact between ITGB1 and *TMEM182* may reduce the binding affinity of ITGB1 for laminin, an important component of the ECM, and thus decrease its interaction with this protein. In addition to modulating the affinity of the ITGB1 protein, direct contact between ITGB1 and *TMEM182* also reduced the activity of ITGB1-mediated intracellular signal transduction, which is essential for *ITGB1* function during myogenesis and muscle regeneration. Thus, our results provided promising evidence of how *TMEM182* acts as a negative regulator of myogenesis (*Figure* 8R) and indicated that the inhibition of *TMEM182* can accelerate muscle growth and regeneration.

Integrins are a superfamily of cell adhesion receptors that are evolutionarily ancient and play important roles during myogenesis and muscle regeneration processes.[21] *ITGB1* is a subunit of the integrin family. *ITGB1* knock-in mice exhibited impaired primary myogenesis and severely reduced skeletal muscle mass.[22] Studies performed in chicks indicated that *ITGB1* is involved in cell migration from the somites and the differentiation of myoblasts into myotubes.[23,24] ITGB1 protein associates with integrin alpha subunits to form integrin complexes that function as ECM receptors. In skeletal muscle, $\alpha7\beta1$ integrin is the major integrin complex that plays roles in many myogenic processes, such as adhesion, migration, cell cycle progression, differentiation, and muscle regeneration.[19,20,25] The interaction between ITGB1 and the ECM is the key determinant of the regulatory function of *ITGB1* in myogenesis. ITGB1 has many binding proteins that can modulate its affinity for ECM ligands.[26–28] Contact between ITGB1 and its binding proteins results in conformational changes in ITGB1 and then reduces the ligand binding affinity.[27] Here, we found another ITGB1-binding protein, the transmembrane protein TMEM182, that can regulate the activity and affinity of ITGB1. There is direct extracellular contact between TMEM182 and ITGB1. TMEM182 binds to an extracellular hybrid domain of ITGB1. A previous study indicated that the conformation of the ITGB1 β-I domain is the key determinant of ligand-binding activity, and the position of the hybrid domain determines the conformational changes.[27,29,30] Direct binding of TMEM182 to the ITGB1 hybrid domain may affect the normal conformational changes in the β-I domain, and then reduce the ligand-binding activity of ITGB1.

Integrin complexes link the intracellular actin cytoskeleton with the ECM and they transmit signals bidirectionally between extracellular ligands and the cytoplasmic domains of integrins.[31] Binding between ITGB1 and the corresponding ECM ligands is associated with the phosphorylation of FAK and then results in the activation of downstream signalling pathways, such as the mitogen-activated protein kinase pathway and PI3K-Akt pathway. The direct contact between ITGB1 and its ligands is important for the activation of ITGB1 mediated downstream pathways. Here, TMEM182 was found to bind to ITGB1 and repress its signal transduction. The phosphorylation of FAK, ERK, and Akt was all decreased in *TMEM182* overexpressing myoblasts, and these proteins and the pathways that they mediate are involved in the regulation of myogenic processes, such as myoblast differentiation, muscle fibre formation, and muscle regeneration. In addition, *ITGB1* was found to rescue the negative effects of

TMEM182 on myogenesis, and *ITGB1* loss of function was found to suppress the inhibitory effects of *TMEM182*. The functions of *TMEM182* in muscle development and muscle regeneration depend on its inhibitory effect on ITGB1 protein function and ITGB1-mediated downstream pathways. Furthermore, *ITGB1* plays an essential role in muscle regeneration. Targeting ITGB1 signalling was found to enhance muscle regeneration in mice.[32] As *TMEM182* is an ITGB1 inhibitor, its repression is a potential therapeutic approach for promoting muscle regeneration and ameliorating muscle atrophy.

To our knowledge, *TMEM182* and *TMEM8C*, which are mainly expressed in muscle tissue, are the only two transmembrane proteins that have been identified to be essential for skeletal muscle development. *TMEM8C* is a vital membrane activator of muscle formation and is essential for muscle regeneration.[9] *TMEM8C* controls myoblast fusion by affecting membrane remodelling, nuclear reprogramming, and cytoskeletal reorganization.[33] However, the detailed mechanism by which *TMEM8C* directly affects these cellular processes remains unclear. Similar to *TMEM8C*, *TMEM182* is critical for muscle formation and muscle regeneration. However, the function of *TMEM182* depends on *ITGB1*, while *TMEM8C* may act independently. Both *TMEM182* and *TMEM8C* are transmembrane proteins. Transmembrane proteins have transmembrane-spanning regions that pass through the lipid bilayer of cell membranes, and the *TMEM182* protein was predicted by Phyre2 to contain four transmembrane spans with the N-terminus and C-terminus in the intracellular space. This structure is similar to that of transmembrane 4 superfamily (TM4SF) proteins, which are associated with integrins in cancer.[34] The TM4SF protein plays important roles in integrin signalling regulation.[35] Several TM4SF proteins act in a manner similar to TMEM182 to direct extracellular binding with ITGB1.[36,37] TM4SF has been implicated in muscle development, myoblast fusion, cell motility, and cell invasion. The ability of a tetraspanin to directly interact with other membrane proteins and form a protein complex to regulate myogenesis or other cellular processes may be a common phenomenon. However, the difference between TMEM182 and the TM4SF proteins and the detailed mechanism of action *TMEM182* remain to be further explored.

In this study, we found that KO of *TMEM182* in mice led to an increase in muscle fibre size, while overexpression of *TMEM182* in chickens resulted in muscle atrophy. However, the detailed mechanism and downstream pathways underlying the regulation of muscle fibre size by *TMEM182* need further investigation. The PI3K-Akt and ERK pathways may be responsible for the function of *TMEM182* in muscle atrophy, because both gain and loss of *TMEM182* function lead to changes in the phosphorylation of Akt, ERK, and FAK. Together, the PI3K-Akt and ERK pathways are the best-known muscle hypertrophy-promoting pathways engaged in integrin-mediated FAK signalling.[38] On the other hand, ITGB1 has many intracellular binding partners that are involved in muscle development and muscle hypertrophy. Can any other pathways or molecules in addition to the FAK-mediated PI3K-Akt and ERK pathways identified in this study be impacted after TMEM182 and ITGB1 interact? It is well known that integrin-linked kinase (ILK) is another important intracellular binding partner of ITGB1 and that integrins can activate Akt and CDC42 in an ILK-dependent manner.[39] By stimulating the phosphorylation of Akt and CDC42, ILK activates several signalling pathways, such as the mTOR, NFkappa-B, cAMP response element-binding protein, and actin cytoskeleton pathways, leading to the expression of cardiac hypertrophic genes and cell migration.[39] Moreover, the results of our Kyoto Encyclopedia of Genes and Genomes pathway analysis (*Figure* S9) indicated the DEGs between the *TMEM182*-KO and WT mice were involved in other pathways, such as the calcium signalling pathway, insulin signalling pathway, and tumour necrosis factor signalling pathway, which are also related to muscle development or muscle hypertrophy. How the interaction between *TMEM182* and ITGB1 affects the activity of these pathways remains to be further studied. In addition, we noted enrichment of many pathways involved in lipid metabolism in the RNA-seq data from *TMEM182*-KO and WT mice (*Figure* S9), and *TMEM182* was specifically expressed in both muscle and fat. Therefore, *TMEM182* may also play important roles in adipogenesis or fat deposition. All the above questions still need to be answered.

Acknowledgements

This work was supported by Natural Scientific Foundation of China (31972544, U1901206 and 31761143014), Guangdong Special Branch Plans of Young Talent with Scientific and Technological Innovation (2019TQ05N470), Natural Science Foundation of Guangdong Province, China (2019A1515010923), the Science and Technology Program of Guangzhou, China (201804020088), the China Agriculture Research System of MOF and MARA (CARS-41), the Local Innovative and Research Teams Project of Guangdong Province (2019BT02N630). The authors of this manuscript certify that they comply with the ethical guidelines for authorship and publishing in the Journal of Cachexia, Sarcopenia and Muscle.[40]

Online supplementary material

Additional supporting information may be found online in the Supporting Information section at the end of the article.

Figure S1. Genes specific expressed in skeletal muscle of chicken

Figure S2. Genes not only specific expressed in skeletal muscle of chicken, but also differentially expressed between myoblast and myotube
Figure S3. qPCR validation of genes differentially expressed between PM, GM, and DM
Figure S4. RNA-seq results of *TMEM182* in different tissues of pig, sheep, and cattle
Figure S5. Ensembl conserved analysis shown that the E-box 1 locate at chicken TMEM182 promoter is conserved among vertebrates
Figure S6. *TMEM182* mRNA expression 48 h after transfection of pcDNA3.1-TMEM182 or si-TMEM182
Figure S7. Conservation analysis of amino acids sequence of TMEM182 protein among vertebrates
Figure S8. PCR validation of TMEM182-KO mice and WT mice
Figure S9. KEGG and GSEA analysis of RNA-seq data from *TMEM182*-KO and WT mice GAS muscle
Figure S10. *TMEM182* KO accelerates muscle regeneration in female mice
Figure S11. Alignment of amino acids sequence of TMEM182 protein among vertebrates. The sequence in the blue box is putative large extracellular domain, and the sequence in the red box is the conserved domain
Figure S12. *TMEM182*, mutated *TMEM182* and *EGFP* overexpression vector were transfected into *ITGB1* knockdown or control myoblasts, and the relative mRNA expression of *TMEM182* and *ITGB1* was analysed
Figure S13. Western blotting of FAK, p-FAK, ERK, p-ERK, AKT1, p-AKT1, and Tubulin for the GAS muscle from *TMEM182*-KO and WT mice
Table S1. DEGs between PM, GM, and DM
Table S2. TMEM182 CoIP result
Table S3. Primers used in this study
Table S4. Gene expression data of RNA-seq from *TMEM182*-KO and WT mice
Table S5. DEGs between *TMEM182*-KO and WT mice

Conflict of interest

None declared.

References

1. Wosczyna MN, Rando TA. A muscle stem cell support group: coordinated cellular responses in muscle regeneration. *Dev Cell* 2018;**46**:135–143.
2. Panda AC, Abdelmohsen K, Martindale JL, Di Germanio C, Yang X, Grammatikakis I, et al. Novel RNA-binding activity of MYF5 enhances Ccnd1/Cyclin D1 mRNA translation during myogenesis. *Nucleic Acids Res* 2016;**44**:2393–2408.
3. Zhang X, Scalf M, Westphall MS, Smith LM. Membrane protein separation and analysis by supercritical fluid chromatography-mass spectrometry. *Anal Chem* 2008;**80**:2590–2598.
4. Kjaergaard M, Kragelund BB. Functions of intrinsic disorder in transmembrane proteins. *Cell Mol Life Sci* 2017;**74**:3205–3224.
5. Dayal A, Ng S, Grabner M. Ca(2+)-activated Cl(−) channel TMEM16A/ANO1 identified in zebrafish skeletal muscle is crucial for action potential acceleration. *Nat Commun* 2019;**10**:115.
6. Yang YD, Cho H, Koo JY, Tak MH, Cho Y, Shim WS, et al. TMEM16A confers receptor-activated calcium-dependent chloride conductance. *Nature* 2008;**455**:1210–1215.
7. Totong R, Schell T, Lescroart F, Ryckebuesch L, Lin Y, Zygmunt T, et al. The novel transmembrane protein Tmem2 is essential for coordination of myocardial and endocardial morphogenesis. *Development* 2011;**138**:4199–4205.
8. Millay DP, O'Rourke JR, Sutherland LB, Bezprozvannaya S, Shelton JM, Bassel-Duby R, et al. Myomaker is a membrane activator of myoblast fusion and muscle formation. *Nature* 2013;**499**:301–305.
9. Millay DP, Sutherland LB, Bassel-Duby R, Olson EN. Myomaker is essential for muscle regeneration. *Genes Dev* 2014;**28**:1641–1646.
10. Luo W, Li E, Nie Q, Zhang X. Myomaker, regulated by MYOD, MYOG and miR-140-3p, promotes chicken myoblast fusion. *Int J Mol Sci* 2015;**16**:26186–26201.
11. Wu Y, Smas CM. Expression and regulation of transcript for the novel transmembrane protein Tmem182 in the adipocyte and muscle lineage. *BMC Res Notes* 2008;**1**:85.
12. Luo W, Wu H, Ye Y, Li Z, Hao S, Kong L, et al. The transient expression of miR-203 and its inhibiting effects on skeletal muscle cell proliferation and differentiation. *Cell Death Dis* 2014;**5**:e1347.
13. Rando TA, Blau HM. Primary mouse myoblast purification, characterization, and transplantation for cell-mediated gene therapy. *J Cell Biol* 1994;**125**:1275–1287.
14. Livak KJ, Schmittgen TD. Analysis of relative gene expression data using real-time quantitative PCR and the 2(-Delta Delta C(T)) method. *Methods* 2001;**25**:402–408.
15. Luo W, Chen J, Li L, Ren X, Cheng T, Lu S, et al. c-Myc inhibits myoblast differentiation and promotes myoblast proliferation and muscle fibre hypertrophy by regulating the expression of its target genes, miRNAs and lincRNAs. *Cell Death Differ* 2019;**26**:426–442.
16. Luo W, Lin S, Li G, Nie Q, Zhang X. Integrative analyses of miRNA-mRNA interactions reveal let-7b, miR-128 and MAPK pathway involvement in muscle mass loss in sex-linked dwarf chickens. *Int J Mol Sci* 2016;**17**:276.
17. Chen B, Xu J, He X, Xu H, Li G, Du H, et al. A genome-wide mRNA screen and functional analysis reveal FOXO3 as a candidate gene for chicken growth. *Plos One* 2015;**10**:e137087.
18. Cao Y, Yao Z, Sarkar D, Lawrence M, Sanchez GJ, Parker MH, et al. Genome-wide MyoD binding in skeletal muscle cells: a potential for broad cellular reprogramming. *Dev Cell* 2010;**18**:662–674.
19. Burkin DJ, Kaufman SJ. The alpha7beta1 integrin in muscle development and disease. *Cell Tissue Res* 1999;**296**:183–190.
20. Crawley S, Farrell EM, Wang W, Gu M, Huang HY, Huynh V, et al. The alpha7beta1 integrin mediates adhesion and migration of skeletal myoblasts on laminin. *Exp Cell Res* 1997;**235**:274–286.
21. Barczyk M, Carracedo S, Gullberg D. Integrins. *Cell Tissue Res* 2010;**339**:269–280.
22. Cachaco AS, Chuva DSLS, Kuikman I, Bajanca F, Abe K, Baudoin C, et al. Knock-in of integrin beta 1D affects primary but not secondary myogenesis in mice. *Development* 2003;**130**:1659–1671.
23. Menko AS, Boettiger D. Occupation of the extracellular matrix receptor, integrin, is a control point for myogenic differentiation. *Cell* 1987;**51**:51–57.
24. Jaffredo T, Horwitz AF, Buck CA, Rong PM, Dieterlen-Lievre F. Myoblast migration specifically inhibited in the chick embryo by grafted CSAT hybridoma cells secreting an anti-integrin antibody. *Development* 1988;**103**:431–446.
25. Liu J, Burkin DJ, Kaufman SJ. Increasing alpha 7 beta 1-integrin promotes muscle cell proliferation, adhesion, and resistance to

apoptosis without changing gene expression. *Am J Physiol Cell Physiol* 2008;**294**: C627–C640.
26. Hadari YR, Arbel-Goren R, Levy Y, Amsterdam A, Alon R, Zakut R, et al. Galectin-8 binding to integrins inhibits cell adhesion and induces apoptosis. *J Cell Sci* 2000;**113**:2385–2397.
27. Campbell ID, Humphries MJ. Integrin structure, activation, and interactions. *Cold Spring Harb Perspect Biol* 2011;**3**.
28. Mazzocca A, Carloni V, Sciammetta S, Cordella C, Pantaleo P, Caldini A, et al. Expression of transmembrane 4 superfamily (TM4SF) proteins and their role in hepatic stellate cell motility and wound healing migration. *J Hepatol* 2002;**37**:322–330.
29. Mould AP, Barton SJ, Askari JA, McEwan PA, Buckley PA, Craig SE, et al. Conformational changes in the integrin beta A domain provide a mechanism for signal transduction via hybrid domain movement. *J Biol Chem* 2003;**278**:17028–17035.
30. Mould AP, Humphries MJ. Regulation of integrin function through conformational complexity: not simply a knee-jerk reaction? *Curr Opin Cell Biol* 2004;**16**:544–551.
31. Schwartz MA, Schaller MD, Ginsberg MH. Integrins: emerging paradigms of signal transduction. *Annu Rev Cell Dev Biol* 1995;**11**:549–599.
32. Rozo M, Li L, Fan CM. Targeting beta1-integrin signaling enhances regeneration in aged and dystrophic muscle in mice. *Nat Med* 2016;**22**:889–896.
33. Zhang Q, Vashisht AA, O'Rourke J, Corbel SY, Moran R, Romero A, et al. The microprotein minion controls cell fusion and muscle formation. *Nat Commun* 2017;**8**:15664.
34. Hemler ME, Mannion BA, Berditchevski F. Association of TM4SF proteins with integrins: relevance to cancer. *Biochim Biophys Acta* 1996;**1287**:67–71.
35. Berditchevski F, Odintsova E. Characterization of integrin-tetraspanin adhesion complexes: role of tetraspanins in integrin signaling. *J Cell Biol* 1999;**146**:477–492.
36. Yauch RL, Kazarov AR, Desai B, Lee RT, Hemler ME. Direct extracellular contact between integrin alpha(3)beta(1) and TM4SF protein CD151. *J Biol Chem* 2000;**275**: 9230–9238.
37. Lozahic S, Christiansen D, Manie S, Gerlier D, Billard M, Boucheix C, et al. CD46 (membrane cofactor protein) associates with multiple beta1 integrins and tetraspans. *Eur J Immunol* 2000;**30**:900–907.
38. Marni D, Ziad S. Integrin signaling: linking mechanical stimulation to skeletal muscle hypertrophy. *Am J Physiol Cell Physiol* 2019;**317**:C629–C641.
39. Lal H, Guleria RS, Foster DM, Lu G, Watson LE, Sanghi S, et al. Integrins: novel therapeutic targets for cardiovascular diseases. *Cardiovasc Hematol Agents Med Chem* 2007;**5**:109–132.
40. von Haehling S, Morley JE, Coats A, Anker SD. Ethical guidelines for publishing in the Journal of Cachexia, Sarcopenia and Muscle: update 2019. *J Cachexia Sarcopenia Muscle* 2019;**10**:1143–1145.